PONTIFICIA UNIVERSIDAD CATÓLICA DEL PERÚ

FACULTAD DE CIENCIAS E INGENIERÍA

REVISIÓN TEÓRICA DE FÍSICA NO-ESTÁNDAR PARA SU INTRODUCCIÓN EN OSCILACIONES DE NEUTRINOS

Tesis para obtener el título profesional de Licenciada en Física

AUTORA

Alicia Pérez García

ASESOR

Alberto Martín Gago Medina

Lima, noviembre, 2020

ET LUX IN TENEBRIS LUCET
MCMXVII

Resumen

Esta tesis contiene al Trabajo de Investigación para Bachillerato presentado en [1], donde se incluyen los capítulos 1, 2 y 3. Estos han sido revisados y corregidos según correspondía. Los capítulos 4, 5 y 6 de este trabajo son contribuciones nuevas.

Los neutrinos juegan un papel importante en nuestro entendimiento de la naturaleza y están siendo estudiados exhaustivamente en la actualidad. En particular, la solución de oscilaciones de neutrinos inducidas por masa está respaldada por contundente evidencia experimental, y presenta un excelente escenario para observar nuevas interacciones con materia. Como un punto de partida en la investigación en Física de Neutrinos, nuestro objetivo es revisar el formalismo de oscilaciones de neutrinos e Interacciones No-Estándar (NSI).

Este trabajo propone la revisión de la descripción en Mecánica Cuántica de las oscilaciones de neutrinos, discutiendo las inconsistencias de las aproximaciones usuales y planteando una más precisa. El mecanismo de oscilaciones en materia también es estudiado con el propósito de derivar las ecuaciones diferenciales a resolver para la evolución de estados.

Además, debido a que su masa puede causarlas, revisamos el marco comúnmente usado de Interacciones No-Estándar de neutrinos con materia y su introducción en las ecuaciones. Los efectos de NSI son considerados en la producción, detección y propagación de neutrinos, particularmente en el contexto de *Deep Underground Neutrino Experiment* (DUNE).

Para encontrar los estados evolucionados, se desarrolló un programa para resolver la ecuación de Schrödinger numéricamente. Los resultados fueron com-

parados con los datos existentes de un software de simulación de experimentos de neutrinos, permitiendo la validación de nuestras soluciones y, de la misma manera, la modificación apropiada del software. Los efectos de las Interacciones No-Estándar son presentadas de manera más evidentes.

Dedicado a Javier Souza

Gracias por todo

Agradecimientos

Quisiera agradecer a mi asesor, Dr. Alberto Gago, no solo por su guía a lo largo del desarrollo de este trabajo, sino también por la confianza puesta en mí. Gracias a los miembros del Grupo de Altas Energías (GAE-PUCP), por la oportunidad de ser parte de su investigación desde el año 2017, y su disposición a responder mis preguntas. A mis amigos, por el constante apoyo y compañía, tanto en nuestra vida académica como fuera de ella.

Agradezco enormemente a mi familia: a mi madre, Laura, por todo el esfuerzo que ha realizado y sigue realizando, sus palabras de aliento y de calma. A mi hermano, Roger, a mis tíos, Yrene y Javier, y a mis abuelos, Ana y Anastacio, por su inagotable cariño, confianza y apoyo incondicional.

Finalmente, quisiera agradecer a la Dirección de Gestión de la Investigación, por brindar financiamiento para esta tesis, a través del Programa de Apoyo al Desarrollo de la Tesis de Licenciatura (PADET) 2019.

Contents

List of Figures

List of Tables

Contents

Chapter 1

Historical Review

To refer to the history of neutrinos is to refer to that of weak interactions, which starts with the discovery of the radioactivity of uranium, and two of its types of products, α and β particles, by Becquerel and Rutherford respectively. In 1914, Chadwick experimentally demonstrated the energy spectrum of electrons emitted in β-decay to be continuous. This fact was controversial, as the beta decay of a nucleus was thought to generate a single particle (an electron) and conservation of energy implies that this particle should have a well-defined energy. In an attempt to solve this problem, conservation of energy was questioned, with N. Bohr suggesting that energy could be conserved only in a statistical sense. However, Pauli proposed the existence of a weakly interacting fermion that was emitted in β-decay [2].

In 1933, Francis Perrin suggested that the new particle, now with the name of neutrino, needed to have a mass smaller than the one of the electron, a velocity close to the speed of light, and spin 1/2. That same year, Fermi formulated a

theory on β-decay [3], establishing the process as:

$$n \rightarrow p + e^{-} + \bar{\nu} \tag{1.1}$$

After these contributions, few doubted the existence of the neutrino, but it was only observed in the 1950s by Reines and Cowan, with their measurement of inverse β-decay ($\bar{\nu} + p \rightarrow n + e^{+}$). For this purpose, they used the flux of anti-neutrinos from a nuclear reactor and 1400 liters of liquid scintillators, constituting the first reactor neutrino experiment.

There are three known neutrino flavors: the electron neutrino ν_e, observed by Reines and Cowan, the muon neutrino ν_μ, first observed in accelerator neutrino experiments (beams made from the reaction $\pi^{+} \rightarrow \mu^{+} + \nu_\mu$, and $\mu^{+} \rightarrow e^{+} + \nu_e + \bar{\nu}_\mu$), and the tau neutrino ν_τ, whose evidence is only inferred from the τ decay modes. In distinction with the other fermions, neutrinos are only sensible to weak interactions: a tiny fraction from a sample of neutrinos in a medium will interact with matter [4].

Apart from nuclear reactors and accelerators, neutrinos can also come from the Sun, atmospheric reactions or extragalactic sources. The Sun releases its energy in nuclear fusion reactions taking place in the solar core, in a network of two-particle reactions, of which the most important one is the pp chain:

$$p + p \rightarrow {}^{2}\mathrm{H} + e^{+} + \nu_e \tag{1.2}$$

We are also led to other neutrino production reactions:

$$^{3}\mathrm{He} + ^{4}\mathrm{He} \rightarrow ^{7}\mathrm{Be} + \gamma \tag{1.3}$$

$$^{7}\mathrm{Be} + e \rightarrow ^{7}\mathrm{Li} + \nu_e \tag{1.4}$$

$$^{7}\mathrm{Be} + p \rightarrow ^{8}\mathrm{B} + \gamma \tag{1.5}$$

$$^{8}\mathrm{B} \rightarrow ^{8}\mathrm{B} + e + \nu_e \tag{1.6}$$

This gives rise to the dominant energy generation mechanism in the Sun [5], and it represents a pure flux of electron neutrinos. Then, experiments at the time detected only electron flavor neutrino. For example, The SAGE and GALLEX experiments made measurements by making solar neutrinos react with gallium, according to:

$$\nu_e + ^{71}\mathrm{Ga} \rightarrow ^{71}\mathrm{Ge} + e^{-} \tag{1.7}$$

While the Kamiokande and Super-Kamiokande experiments used the reaction:

$$\nu_e + e^{-} \rightarrow \nu_e + e^{-} \tag{1.8}$$

with an energy threshold of 5 MeV in a water Cherenkov counter. However, the observations did not give fluxes as great as the one predicted by the solar standard model for solar neutrinos [6]. This resulted in the so-called *solar neutrino problem*: there seemed to be a loss in the flux on the neutrinos way to Earth.

To solve the solar neutrino problem, many proposals were made, from doubting the correctness of the standard solar model, doubting the estimation of the

cross-section for the reactions in the experiments, to assuming that neutrinos could decay into new particles that would be invisible to detectors. As these scenarios are fairly unlikely, neutrino oscillations, along with its resonances due to the presence of a heavily dense medium, could also offer an explanation about the mechanism that causes the solar neutrino problem. The difference between the measured and the predicted neutrino fluxes was solved by the SNO experiment. It was able to measure different neutrino flavors by using their reactions with a deuteron:

$$\nu_e + d \rightarrow p + p + e^- \tag{1.9}$$

$$\nu_x + d \rightarrow p + n + \nu_x \tag{1.10}$$

The total neutrino flux it obtained was in agreement with the predicted flux, even if the mechanism for this result is not clear [7].

Having formerly been unwanted background for experiments, atmospheric neutrinos have provided the first indication for neutrino oscillations. The mechanism for muon production in the atmosphere from Cosmic Rays is known and accepted. A charged particle from an extragalactic source arrives at the Earth's atmosphere and interacts with nuclei there, causing both an electromagnetic and a hadronic shower. From the latter, pions are produced and they then decay, as mentioned in the accelerator experiments case. Thus, giving an expectation of a ratio of 2 to 1 between the number of ν_μ and the number of ν_e. Once again, the measured flux was not in agreement with the theoretical prediction, until Super-Kamiokande measured not only the energy of the neutrinos, but their di-

rection, and, indirectly, the differences in their traveled path. It was found that the neutrino flavor transition was actually dependent on this length [8].

Based on these observations, the most accepted theory was that of a periodic change in neutrino flavor, induced by their mass differences. Following the $K_0 - \bar{K}_0$ particle system, Pontecorvo suggested that oscillations happened because the flavor eigenstates did not have a defined mass, but were a quantum superposition of mass states (the eigenstates of the corresponding evolution operator). Both bases were related by a rotation angle, θ, given by nature, and this formulation gave rise to the usual approach to neutrino oscillations, which will be described in more detail in the following chapter.

Chapter 2

Description of Neutrino Oscillations

2.1 The typical approach

To describe the change in neutrino flavor as it propagates through space, it is necessary to notice first that flavor states are not energy (mass) eigenstates. Therefore, they are not the evolution operator eigenstates, and propagation cannot be understood directly from them. Nevertheless, the energy eigenstates constitute a basis and can be used to write a given flavor as a superposition of them:

$$|\nu_\alpha\rangle = \sum_i U_{\alpha i} |\nu_i\rangle \tag{2.1}$$

$$|\nu_\alpha(t)\rangle = \sum_i U_{\alpha i} e^{-iHt} |\nu_i\rangle \tag{2.2}$$

The evolution operator is then applied on the mass eigenstates and the energy is obtained for each one of them, according to the energy-momentum relation $E^2 = p^2 + m^2$. For example, for the particular case of two generation mixing, where U represents a rotation matrix that depends on a parameter from nature,

θ:

$$U = \begin{pmatrix} \cos\theta & -\sin\theta \\ \sin\theta & \cos\theta \end{pmatrix} \tag{2.3}$$

Each mass state $|\nu_i\rangle$ has an energy E_i, and the evolved flavor state is:

$$|\nu_\alpha(t)\rangle = e^{-iE_1 t}\cos\theta\,|\nu_1\rangle - e^{-iE_2 t}\sin\theta\,|\nu_2\rangle \tag{2.4}$$

Then, the transition probability from the initial neutrino flavor α into a flavor β is:

$$P_{\nu_\alpha\to\nu_\beta} = \sin^2 2\theta \sin^2\left[\frac{(E_2 - E_1)}{2}t\right] \tag{2.5}$$

The energies involved in the probability formula can be expressed using the relativistic approximation:

$$E_i = \sqrt{p_i^2 + m_i^2} \tag{2.6}$$

$$E_i \simeq p_i + \frac{m_i^2}{2p_i} \tag{2.7}$$

The use of this approximation is completely justified: the current boundaries for neutrino masses indicate that they are less than 1 eV and their energy needs to be higher than 100 keV to be detected. This bears a tiny ratio of $\frac{\Delta m^2}{p^2} \leq 10^{-10}$ [9].

We can then introduce this into Eq. (2.5) and make $t = L$. We may also consider that, as neutrinos are ultra relativistic, $p_i = E_i$ and $p_1 = p_2 = E$. Thu we obtain the master formula for two generations:

$$P_{\nu_\alpha\to\nu_\beta} = \sin^2 2\theta \sin^2\left(\frac{\Delta m^2}{4E}L\right) \tag{2.8}$$

For three generation oscillations, the mixing matrix becomes more complex:

$$U_{PMNS} = \begin{pmatrix} c_{12}c_{13} & s_{12}c_{13} & s_{13}e^{-i\delta_{CP}} \\ -s_{12}c_{23} - c_{12}s_{23}s_{13}e^{i\delta_{CP}} & c_{12}c_{23} - s_{12}s_{23}s_{13}e^{i\delta_{CP}} & s_{23}c_{13} \\ s_{12}s_{23} - c_{12}c_{23}s_{13}e^{i\delta_{CP}} & -c_{12}s_{23} - s_{12}c_{23}s_{13}e^{i\delta_{CP}} & c_{23}c_{13} \end{pmatrix} \tag{2.9}$$

where $c_{mn} = cos\theta_{mn}$, $s_{mn} = sin\theta_{mn}$ and δ_{CP} is a CP-violating phase. Obtaining a master formula for three generation mixing becomes considerably more difficult.

Although the steps followed for obtaining the probability formulas work well and are in fact widely used experimentally, notation should be able to describe the space-time and energy-momentum degrees of freedom for a neutrino state, by factorizing the general states as described in [9]: considering that the aforementioned quantities are not certainly known for flavor states, only mass states can be written by defining the complete Hilbert space $\mathscr{H}$ as the product of a space corresponding to the momentum and another one, to the mass of the neutrino.

$$\mathscr{H} := \mathscr{H}_d \otimes \mathscr{H}_m \tag{2.10}$$

Thus, a general neutrino mass state $|\nu_i\rangle \in \mathscr{H}$ will have definite kinematical properties [10] and will be expressed as:

$$|\nu_i\rangle := |\nu_i^m\rangle \otimes |p_i\rangle \tag{2.11}$$

and a flavor state can be written as:

$$|\nu_\alpha\rangle = \sum_i U_{\alpha i} |\nu_i^m\rangle \otimes |p_i\rangle \tag{2.12}$$

The wave function for this initial neutrino flavor state is:

$$|\nu_\alpha(\vec{x})\rangle = \langle\vec{x}|\nu_\alpha\rangle = \sum_i U_{\alpha i} e^{i\vec{p}_i\cdot\vec{x}} |\nu_i^m\rangle \tag{2.13}$$

Now, we can apply the evolution operator to the state, and the neutrino flavor state for a time t and position $\vec{x}$ becomes:

$$|\nu_\alpha(t,\vec{x})\rangle = \sum_i U_{\alpha i} e^{-iE_i t} e^{i\vec{p}_i\cdot\vec{x}} |\nu_i^m\rangle = \sum_i U_{\alpha i} e^{-ip_i x} |\nu_i^m\rangle \tag{2.14}$$

Finally, the transition probability of the initial flavor α into a flavor β, defined by $\left|\langle\nu_\beta|\nu_\alpha(t,\vec{x})\rangle\right|^2$, depends on the phase differences between mass states:

$$\Delta\phi_{ik} = \Delta E_{ik}\cdot t - \Delta\vec{p}_{ik}\cdot\vec{x} \tag{2.15}$$

2.2 Approximations and their accuracy

To evaluate Eq. (2.15), some assumptions are usually made, just as done for obtaining 2.8, and as will be described below. The analysis in the following sections will be based on the work in [11], summarizing and specifying some details.

1. Same momentum: By establishing $p_i = p_k = p$, the space dependence of the phase difference vanishes, and the oscillation probability depends only

on time and energy. According to the relativistic approximation, Eq. (2.7), we obtain:

$$\Delta\phi_{ik} \simeq \frac{\Delta m^2_{ik}}{2p} t \tag{2.16}$$

Now, the distance between source and detector is known much more accurately than the time of propagation in neutrino experiments. This is handled here by making the time to space conversion: as neutrinos are considered to be ultra-relativistic, $L \simeq t$ and

$$\Delta\phi_{ik} \simeq \frac{\Delta m^2_{ik}}{2p} L \tag{2.17}$$

2. Same energy: As neutrinos are created in weak interactions, they have a well-defined flavor at their source, and it is only necessary to examine the behavior of a single energy state: oscillation probabilities can be found by evaluating a linear superposition of mass states with same energy and different momenta [12]. Following this argument, using the same energy for all mass states ($\Delta E = 0$) in Eq. (2.15) is also a common approach. It is also possible to consider $\vec{x}||\vec{p}$, as the distance from source to the detector is much larger than the transverse sizes [11]. By also applying an approximation analogous to Eq. (2.7), the oscillation phase is:

$$\Delta\phi_{ik} = -\Delta p_{ik} \cdot L \simeq \frac{\Delta m^2_{ik}}{2E} L \tag{2.18}$$

Inconsistencies can be found in the approaches, as several contradictions arise. It is first necessary to establish some aspects regarding the observability of

oscillations in experiments:

a) The processes of neutrino production and detection are localized and have different coordinates in space, so we must be able to distinguish positions.

b) Transition probabilities must depend on space coordinates.

c) The production and detection of neutrinos also happen at specific instants in time.

d) The phenomenon of neutrino oscillations is the result of quantum interference, due to momentum (space) and energy (time) uncertainties. Therefore, our description must account for them.

Let us first recall Eq. (2.16). The probability will not depend on any spatial coordinates, so same momentum assumption cannot define production and detection regions, contradicting aspect a). Moreover, a time-only dependence of the phase difference could lead us to believe that detecting neutrinos, for example, at their source would be sufficient to observe oscillations. This contradicts the definition of flavors by the weak charged current. However, the approach arrives at supporting aspect b) by using the time to space conversion. Note here that the latter can only be applied if there is a classical velocity (for a point-like particle) [11].

Assuming that the neutrino mass states all have the same momentum means that it is well-defined -i.e., they are momentum eigenstates and their wave functions in momentum space are delta functions:

$$\psi_i(\vec{p}) = \delta(\vec{p} - \vec{p}_i) \tag{2.19}$$

In the position space, this wave function becomes:

$$\psi_i(\vec{x},t) = \frac{1}{(2\pi)^{\frac{3}{2}}} e^{i\vec{p}\cdot\vec{x} - iE_i t} \tag{2.20}$$

The same momentum assumption then leads us to consider the wave functions as plane waves with definite $\vec{p}_i$ [9]. A group velocity cannot be defined for plane waves, but it is the equivalent to a point-like particle velocity, used for the time to space conversion. Therefore, we arrive at an internal inconsistency of the approach.

Finally, plane waves do not account for energy-momentum spread, which contradicts aspect d). The oscillation phenomenon would not be possible with plane waves.

The same energy approach results in a phase difference that does not account for the time dependence of oscillations, and contradicts aspect c). Furthermore, it could be argued that same energy for the mass states can be a reality for certain Lorentz frames. Let us follow the logic in [13], and assume there is a Lorentz frame $\mathscr{O}$ where all neutrino mass states have the same energy $E_i = E$ and, of course:

$$p_i \simeq E - \frac{m_i^2}{2E} \tag{2.21}$$

If we now consider another frame $\mathscr{O}'$, with a velocity v along the x axis with respect to $\mathscr{O}$. The energy E then becomes:

$$E_i' = \gamma(-v p_i + E) \tag{2.22}$$

$$E_i' \simeq \sqrt{\frac{1-v}{1+v}}E + \frac{v}{\sqrt{1-v^2}}\frac{m_i^2}{2E} \tag{2.23}$$

Defining a quantity E', which will be a term common to E and p of all neutrino mass states (as it depends on E and v), we get:

$$E_i' \simeq E' + \frac{v}{1+v}\frac{m_i^2}{2E'}, \tag{2.24}$$

where

$$E' = \sqrt{\frac{1-v}{1+v}}E \tag{2.25}$$

By applying the Lorentz transformation to p_i as well:

$$p_i' = E' - \frac{1}{1+v}\frac{m_i^2}{E'} \tag{2.26}$$

In general, the energy and momenta of mass eigenstates would not be equal when changing frames. More specifically:

$$\Delta E_{ij}' = \frac{v}{1+v}\frac{\Delta m_{ij}^2}{2E'}, \quad \Delta p_{ij}' = -\frac{1}{1+v}\frac{\Delta m_{ij}^2}{2E'} \tag{2.27}$$

The same energy approach then is not universal, and cannot be supported with any physical arguments: it will not work simultaneously for different experimental conditions. Moreover, even if we found a frame where energies are the same (where they are determined by the production process and have no dependence on neutrino mass), it would not be particularly useful. Let us consider the pion decay, $\pi^+ \to \mu^+ \bar{\nu}_\mu$.

Kinematic treatment to this case, considering massless neutrinos, gives for the energy of $\bar{\nu}_\mu$:

$$E_\nu = \frac{m_\pi}{2}\left(1 - \frac{m_\mu^2}{m_\pi^2}\right) \tag{2.28}$$

This is the zeroth order approximation, that would consider $p_i = E_i = E$. However, there are in fact mass contributions. The kinematic treatment when considering neutrino mass, gives:

$$E_i \simeq E + (1-\xi)\frac{m_i^2}{2E}, \tag{2.29}$$

where

$$\xi = \frac{1}{2}\left(1 + \frac{m_{\mu^2}}{m_\pi^2}\right) \tag{2.30}$$

Thus, energy for the mass states will differ according to the Lorentz frame considered for production. Of course, they could have the same energy if we consider a boosted reference frame, i.e., for the case where a decaying particle is not at rest, where we can arrive at a parameter $\xi' = \xi'(\xi, v) = 1$. Nevertheless, this frame does not coincide with the laboratory frame, meaning it is not useful for calculations and predictions, and would depend on the energy of the decaying particle. In realistic conditions, particle beams are not monochromatic, and the non-existence of one single value for the energy means that the boost needed to arrive at the desired reference frame is not unique.

2.3 An accurate treatment

As established in the previous section, plane waves cannot describe localized neutrino production and detection, or a single localized particle for that matter. In general, the latter is usually described by a wave packet: a superposition of plane waves. Additionally, a wave packet has a momentum spread σ_p around a central momentum $\vec{p}_0$, as the uncertainty relation implies that, if we have a localized state in space, then we can know its momentum only with an uncertainty $\sigma_p \gtrsim \frac{1}{\sigma_x}$ [2]. The individual plane waves that compose a wave packet each have a value for their respective momentum that is in fact close to the central value $\vec{p}_0$, determined by the production and detection processes.

Just by examining the definition of wave packet, we see that it is in agreement with the aspects for oscillation observability, thus validating the use of wave packets for describing the states. Let us take a closer look at this formalism.

Using the wave packet approach, a particle of mass m_i is represented in the coordinate space by a wave function of the form:

$$\Psi(\vec{x},t) = \int \frac{d^3p}{(2\pi)^3} f_{\vec{p}_0} \exp(i(\vec{p}\cdot\vec{x} - E_i(p)t)) \tag{2.31}$$

where $f_{\vec{p}_0}$ is the corresponding momentum distribution with a peak at $\vec{p}_0$, momentum spread σ_p and, of course, energy given by the dispersion relation, Eq. (2.6). Then, the evolved state for the neutrino flavor in Eq. (2.14) becomes:

$$|\nu_\alpha(t,\vec{x})\rangle = \sum_i U_{\alpha i} \Psi_i(t,\vec{x}) \, |\nu_i\rangle \tag{2.32}$$

and any other flavor states $|\nu_\beta\rangle$ must also be described by an Eq.(2.32)-type expression [11].

Let us now evaluate the oscillation phase. Keep in mind that neutrinos are not only relativistic, but also almost degenerate in mass: We can consider that the different mass states have energy and momentum differences be very small compared to the average values, i.e, $\Delta E_{ij} \ll E_{average}$ and $\Delta p_{ij} \ll p_{average}$.

We can, in general, expand the energy of one mass state i as:

$$E_i(\vec{p}) = E_i(\vec{\tilde{p}}_i + \Delta\vec{p}) = E(\vec{\tilde{p}}_i) + \frac{\partial E}{\partial p}\Big|_{\tilde{p}_i} |\Delta\vec{p}|, \tag{2.33}$$

where $\vec{\tilde{p}}_i$ is the average momentum of the mass state and $\Delta\vec{p} = \vec{p} - \vec{\tilde{p}}_i$. Our state is a wave packet composed of a main wave and modulations to it, which all have a velocity:

$$v_{g,i} = \frac{\partial E}{\partial p}\Big|_{\tilde{p}_i} \tag{2.34}$$

If we consider, for simplicity, that $v_{g,i} = v_g$ is universal and $\vec{\tilde{p}}$ is the overall average value of $\vec{p}$ (remember the value of $\vec{\tilde{p}}_i$ is much larger that its difference with other $\vec{\tilde{p}}_j$), we can obtain:

$$\Delta E_{ik} = v_g |\Delta\vec{p}_{ik}| + \frac{1}{2|\vec{\tilde{p}}|}\Delta m^2_{ik} \tag{2.35}$$

Let us notice that this newly defined group velocity can be used for establishing relations of the form $x = vt$, as it is interpreted as the velocity of the localized particle described by our wave packet. Thus, allowing us to make use of time to space conversion $t = L/v_g$ with no contradictions.

If we introduce Eq. (2.35) into the phase difference found at first, Eq. (2.15),

we can obtain two possible new expressions for the latter:

$$\Delta\phi_{ik} = \Delta E_{ik} \cdot t - \Delta\vec{p}_{ik} \cdot \vec{x} = \Delta E_{ik} \cdot t - \Delta p_{ik} L \tag{2.36}$$

$$\Delta\phi_{ik} = (v_g t - L)\Delta p_{ik} + \frac{1}{2|\vec{\tilde{p}}|^2} E L \Delta m^2_{ik} \tag{2.37}$$

$$\Delta\phi_{ik} = \frac{1}{v_g}(v_g t - L)\Delta E_{ik} + \frac{1}{2|\vec{\tilde{p}}|^2} E L \Delta m^2_{ik} \tag{2.38}$$

Note that for Eq. (2.37) and Eq. (2.38), we are considering $L = v_g t$ and $v_g = |\vec{\tilde{p}}|/\tilde{E}$ (the same for all mass states), and $\tilde{E}$ is the average energy of the mass states. We may take it a little further with the assumption of ultra-relativistic neutrinos and consider $v_g \to 1$ and $|\vec{\tilde{p}}| \to E(\vec{\tilde{p}})$. Then, we can conveniently arrange our phase differences:

$$\Delta\phi_{ik} = (v_g t - L)\Delta p_{ik} + \frac{1}{2\tilde{E}} L \Delta m^2_{ik} \tag{2.39}$$

$$\Delta\phi_{ik} = \frac{1}{v_g}(v_g t - L)\Delta E_{ik} + \frac{1}{2|\vec{\tilde{p}}|} L \Delta m^2_{ik} \tag{2.40}$$

Both Eq. (2.39) and Eq. (2.40) can have their first term on the right hand side vanish only for the case of the center of the wave packet, where $v_g t = L$. However, other positions cannot have a distance to the center of over σ_x to it:

$$\left|v_g t - L\right| \leq \sigma_x \tag{2.41}$$

and we can establish a condition for each expression so their first term vanishes:

$$\sigma_x \left|\Delta p_{ik}\right| \ll 1 \tag{2.42}$$

$$\frac{\sigma_x}{v_g}|\Delta E_{ik}| \ll 1 \tag{2.43}$$

Let us also recall that Heisenberg's uncertainty indicates that $\sigma_x \sim \frac{1}{\sigma_p}$, so our condition in Eq. (2.42) becomes:

$$|\Delta p_{ik}| \ll \sigma_p \tag{2.44}$$

From $E^2 = p^2 + m^2$, we can obtain $\sigma_E = \frac{p}{E}\sigma_p = v_g\sigma_p$. Then, the uncertainty principle also implies $\sigma_x \sim \frac{v_g}{\sigma_E}$, and the condition in Eq. (2.43) becomes:

$$|\Delta E_{ik}| \ll \sigma_E \tag{2.45}$$

If the relations in Eq. (2.44) and (2.45) hold for the mass states, the phase differences found with the same momentum and same energy assumptions are recovered: The approximations are justified (and correct) as long as the differences in energy and momentum between the mass states are much smaller than their corresponding quantum uncertainty. The mass contribution to the energy and momentum of each massive neutrino needs to be very small to allow all E_i and p_i to be very close in value. In fact, so close that we may confuse them due to quantum fluctuations.

2.4 Uncertainties and coherence

It is not a coincidence that our conditions for justifying the approaches are related to quantum uncertainties. In fact, they are the reason for the entire phenomenon, apart from just the use of quantum mechanics in the description:

Eq. (2.44) and (2.45) are the so-called *coherence conditions* that allow neutrino oscillations to be observable.

Let us take a look at a pion decay, $\pi^+ \to \mu^+ \nu_\mu$, and follow the standard procedure of 4-momentum conservation ($P_\pi = P_\mu + P_\nu$). Applying this for the case in which the pion is not at rest, we can express the mass of the neutrino in terms of the masses and momenta of the pion and muon. If the experiment to be performed were able to precisely measure the momenta, it would be able to determine the neutrino mass squared m_ν^2 and distinguish it from the other neutrino masses, as described below, following [14].

If we consider that the experiment will detect only a specific neutrino flavor, the rate of the events of a particular neutrino mass state will be proportional to the probability to trigger detection and the probability for a pion to decay in the muon channel. Therefore, the results will depend on how a neutrino flavor state is a superposition of mass states, but not vary with spatial coordinates: there will be no oscillation pattern.

This can be explained as follows: if the experiment can determine E and p with independent errors, the dispersion relation can be used to find an uncertainty for the neutrino mass squared:

$$\sigma_{m^2} = \sqrt{[2E\sigma_E]^2 + [2p\sigma_p]^2} \tag{2.46}$$

For a mass state to be identified, it is necessary that $\Delta m^2 > \sigma_{m^2}$. For this to hold, we see from Eq. (2.46) that we need:

$$2p\sigma_p < \Delta m^2 \tag{2.47}$$

and by using the uncertainty principle, we arrive at:

$$\sigma_x > \frac{2p}{\Delta m^2} \tag{2.48}$$

Before continuing, we need to define a relevant quantity: the oscillation length. Eq. (2.14) can be expressed using Eq. (2.7) as:

$$|\nu_\alpha(t,\vec{x})\rangle = \sum_i U_{\alpha i} e^{-i\frac{m_i^2}{2p}t} |\nu_i^m\rangle \tag{2.49}$$

The probability of measuring a state given by Eq.(2.13), using time to space conversion, is then [14]:

$$P_{\nu_\alpha \to \nu_\beta} = \sum_i U_{\alpha i}^2 U_{\beta i}^2 + \sum_{i \neq j} U_{\alpha i} U_{\beta i}^* U_{\alpha j}^* U_{\beta j} \cos(x\frac{\Delta m^2}{2p}), \tag{2.50}$$

As the periodicity of the cosine is given by 2π, we can write the term as $cos(2\pi\frac{x}{l_{osc}})$, where

$$l_{osc} = 2\pi\frac{2p}{\Delta m^2} \tag{2.51}$$

is the oscillation length for our probability. Except for a factor of 2π, this is precisely the condition stated in Eq. (2.48).

We can now interpret the disappearance of oscillations with precise momentum measurements. As the pion momentum is more accurately defined, its position will be more undetermined and the neutrino production will be delocalized [14]. When the pion momentum is measured with enough precision such that σ_{m^2} is less than all Δm^2, the uncertainty in the coordinate of the production point exceeds the oscillation length and oscillations are averaged. For example, for an

experiment with average momentum $p = 2.5$ GeV and assuming only $\Delta m^2_2 1 = 7.2 \times 10^{-5}$ eV^2, we would have $l_{osc} \simeq 4.36 \times 10^9$ eV$^{-1} = 5.41 \times 10^8$ m. If we could not localize our production point within 500000 km, we would not observe oscillations.

Even though this entire argument was made by taking into account only the production of a neutrino, it can be similarly done for neutrino detection. Thus, we have arrived at a condition for the observability of oscillations: we must not be able to distinguish what mass state has been produced or detected. This condition is satisfied only if neutrino production and detection have their spatial coordinates well-defined (they have small values for σ_x).

It could be argued that this violates energy-momentum conservation. However, given that neutrinos (and their processes) have spatial and time coordinates with their respective uncertainties, so do their energy and momentum values. Then, the states that represent our particles are not exactly eigenstates of energy and momentum, but this does not imply the 4-momentum is not conserved [11].

Another formulation for the coherence conditions can be done in configuration space and arrive at conditions that are in agreement with the discussion so far. For that, we focus on the fluctuations of the oscillation phase, which must be small as not to average the probability over the oscillation phase:

$$|\delta\phi| = |\Delta E \cdot \delta t - \Delta\vec{p} \cdot \delta\vec{x}| \ll 1 \tag{2.52}$$

If we assume that in no frame will the terms in Eq. (2.52) cancel (or rather if we are not looking to get Lorentz invariant conditions), both terms need to be

small on their own. Furthermore, the fluctuations in, for example, production position and time are, at most, equal to the uncertainties of those quantities, $\delta t \lesssim \sigma_t$ and $|\delta\vec{x}| \lesssim \sigma_x$. All these relations finally arrive at [11]:

$$|\Delta E| \ll \sigma_E \tag{2.53}$$

$$|\Delta p| \ll \sigma_p \tag{2.54}$$

These are the exact same conditions assumed for evaluating the oscillation phase in the wave packet approach, and support the role of the quantum uncertainties in observing oscillations.

While we have established that coherence in production and detection is needed for neutrino oscillations to be observed, this condition is not sufficient by itself. For a given momentum, the waves for each mass state will travel at different speeds v_g, as they depend on the respective mass, resulting in the separation of their centers. When the waves do not overlap, the mass states cannot interfere and produce oscillations [14] and so, coherence is lost.

However, the waves will maintain coherence while travelling some distance in space, called the coherence length. Its value can be deduced logically from the conditions already mentioned. Let us consider an average group velocity for the mass states, v_g, and the average distance traveled by the different waves, $l = v_g t$. The separation between mass states after a time t will be given by $\Delta l = \Delta v_g t$, and for there to be interference of the states, this separation must be less than the wave spatial spread σ_x, or at most, equal to it after a time $t_{coh} = \frac{l_{coh}}{v_g}$. As a

result of these equations, the coherence length is found to be:

$$l_{coh} \simeq \frac{v_g}{|\Delta v_g|}\sigma_x \tag{2.55}$$

Considering ultra relativistic neutrinos, we can use $p \sim E$ and $v_g \simeq 1$. Also, by considering an average energy, $\Delta v_g \simeq \frac{\Delta p}{E} \simeq \frac{\Delta m^2}{2E^2}$, and the coherence length is:

$$l_{coh} \simeq \frac{2E^2}{|\Delta m^2|}\sigma_x \tag{2.56}$$

Neutrino oscillations can be observed only for distances traveled that satisfy $L \ll l_{coh}$, which is in fact very large [11]. Let us try again our example of an experiment with average energy $E = 2.5$ GeV and $\Delta m^2_21 = 7.2 \times 10^{-5}$ eV^2, with $\Delta E = 0.5$ GeV. We would then obtain $l_{coh} \simeq 1.39 \times 10^{14}$ eV$^{-1} = 1.72 \times 10^8$. Coherence is then lost in a distance much larger than the radius of the Earth itself.

Even if it seems very difficult not to achieve, if this condition is not met, the detection process will be able to distinguish each mass state wave as they arrive at different times. However, depending on the characteristics of the detection, coherence could be restored.

If the detection process takes longer than the time it takes all the wave packets to arrive to the detection point, there may still be a coherent event. Hence, the coherence length must have a dependence on the time resolution of the detector [15]. From $l = v_g t$, we can obtain:

$$\sigma_x = \sqrt{\left(\frac{\partial l}{\partial v_g}\right)^2 \sigma^2_{v_g} + \left(\frac{\partial l}{\partial t}\right)^2 \sigma^2_t} \tag{2.57}$$

The same approach for finding σ_{v_g} gives a quantity of the order of σ_E/E, so it is vanishingly small. Thus, we get $\sigma_x = v_g\sigma_t = v_g/\sigma_E$, interpreted as an effective length of the wave packet by taking into account the uncertainties of both production and detection [11]. Then, for example, if the energy measurement in the experiment became extremely accurate, the effective length of the wave packet would be infinite, and so would the coherence length: the propagation of the neutrino mass states would not cause the loss of coherence.

2.5 Summarizing the coherence conditions

Neutrino oscillations are observable only if the neutrino flavor state is a coherent superposition the mass states at all times: production, propagation and detection of neutrinos are coherent. There is, however, a possible contradiction among the conditions this sets.

Going back to the example of a very accurate measurement of energy in the detection process, it would not allow the condition in Eq. (2.53) to be satisfied. Furthermore, it would imply an infinitely large uncertainty in time, so the instant for the detection is completely undefined, contradicting the same argument as the same energy approach.

Let us try and evaluate how both coherence conditions could work together. They can be expressed as:

$$\Delta E \sim \frac{\Delta m^2}{2E} \ll \sigma_E \tag{2.58}$$

$$\frac{\Delta m^2}{2E^2} L \ll \frac{v_g}{\sigma_E} \tag{2.59}$$

and would represent limits for σ_E [11]:

$$\frac{\Delta m^2}{2E} \ll \sigma_E \ll \frac{2E^2}{\Delta m^2 L}, \tag{2.60}$$

where v_g has been maximized ($v_g \simeq 1$). The stated relation between the limits will work as long as Δm^2 is small (this explains why neutrinos oscillate, while charged leptons do not). Moreover, by taking only the extremes:

$$2\pi \frac{L}{l_{osc}} \ll \frac{2E^2}{\Delta m^2} \tag{2.61}$$

This ensures the compatibility of the conditions, while not necessarily the fulfillment of both coherence conditions. From Eq.(2.60), we can also get:

$$\frac{L}{l_{osc}} \sim \frac{E}{2\pi\sigma_E} \tag{2.62}$$

Experimentally, σ_E is actually the energy resolution of the detector, which is larger. This establishes conditions to be considered in experiment design, such as the maximum number of observable oscillations, $\frac{l_{coh}}{l_{osc}}$, and the baseline.

2.6 Some remarks

The conditions for neutrino oscillations to occur and be observable discussed so far have a dependency on the production and detection processes. For example, in Eq. (2.31), the neutrino mass state has a dependence on a momentum distribution, which will be different for the neutrino states in production, $\left|f^P_{\vec{p}_0}\right|^2$, and detection, $\left|f^D_{\vec{p}_0}\right|^2$. On the other hand, a flavor state needs to be normalized.

Then, for that to be ensured, they need to satisfy:

$$\int \frac{d^3p}{(2\pi)^3} \left| f^P_{\vec{p}_0} \right|^2 \left| f^D_{\vec{p}_0} \right|^2 = 1 \tag{2.63}$$

So, for probabilities to even make sense, the production and detection processes need to be taken into account. Notice that the integral represents the degree of overlap between the momentum spectra of produced and detected neutrinos, which will, in the end, give the detection efficiency. Of course, this does not mean the overlap will always give 1 and solve the normalization problem. Furthermore, oscillations are a phenomenon in nature, and not induced from experimental conditions, i.e., the oscillation probabilities found with the formalism have to be universal.

Of course, measurable quantities do need to consider the experimental aspects of production, propagation and detection, and they can be represented by the probability of the complete process. If this probability can be expressed as factors of flux (production), interaction probability (detection) and the experiment-independent probability, then we could be able to obtain universal probabilities [11]. This type of factorization will only be possible if all three aspects are independent of each other.

Propagation and detection of the neutrino states will not be dependent of each other. They will also not depend on the production process if the latter generates neutrinos with the same kinematics, which happens if the mass of different states does not affect the momentum. This can all be reduced to having the production process not be able to discriminate between mass states: production

must be coherent. On that note, propagation and detection must also not distinguish masses, so the already established conditions ensure independence for experiments as well.

Finally, universality also implies that the probabilities do not depend on the frame of reference used. The phase difference that defines the probability explicitly includes the relation $\frac{L}{E}$ and, it can be shown that the relation remains invariant. Following the treatment in [16], let us assume an inertial reference frame $\mathscr{O}'$ moving with velocity v in the x direction with respect to another reference frame $\mathscr{O}$, and recall the Lorentz transformations for space and time:

$$\Delta x' = \gamma(\Delta x - v\Delta t) \tag{2.64}$$

$$\Delta t' = \gamma(-v\Delta x + \Delta t) \tag{2.65}$$

where the parameter $\gamma = 1/(1-v^2)$. The distance between the neutrino source and the detector measured in $\mathscr{O}'$ is:

$$L' = \frac{L}{\gamma} \tag{2.66}$$

and the transformations for momentum and energy are:

$$p' = \gamma(p - vE) \tag{2.67}$$

$$E' = \gamma(-vp + E) \tag{2.68}$$

Notice that, if we consider the ultra-relativistic limit in $\mathscr{O}$, we would have the same condition under the boost to get to $\mathscr{O}'$: Having $E = p$ allows us to get the

same expressions for Eq.(2.67) and Eq.(2.68), and the ultra-relativistic limit remains under boosts. Thus, we can also consider it for $\mathscr{O}'$ and obtain:

$$E' = p' = \gamma(1-v)E \tag{2.69}$$

Evidently, L' and E' will not result in probabilities equal to the ones using L and E. However, for obtaining our phase difference, we have used the approximation of $L = t$. The parameter L does not represent the distance between the source and detector, but rather the distance traveled by the neutrino. On one hand, we have for $\mathscr{O}$, $\Delta x = \Delta t$, and for $\mathscr{O}'$:

$$\Delta x' = \Delta t' = \gamma(1-v)\Delta x \tag{2.70}$$

Then, the correct transformation for L is:

$$L' = \gamma(1-v)L \tag{2.71}$$

The relation L'/E' can now be seen to be equal to L/E [16]. That being the case, probabilities now can be considered as universal.

Chapter 3

Oscillations in Matter

So far, we have established an acceptable formalism for neutrino oscillations and found arguments to support the more simple approaches, as the necessary conditions are usually satisfied. This has been done by only taking into account the properties of the particles themselves, without any additional potentials from the medium they are in -i.e., we have considered neutrino oscillations in vacuum.

According to the Standard Model, neutrinos have no mass and are left-handed, which allows them to interact only through weak force. On the other hand, we have so far assumed that the reason for the oscillation phenomenon to occur is that neutrinos are not actually massless, giving us a hint for new physics, which will be considered in following chapters. For the purpose of the present chapter, we will consider only the standard interactions via weak force, through either charged or neutral currents. Even though their interaction rate is relatively low, oscillations can be affected when considering neutrinos in a medium, in the presence of nucleons and electrons. The introduction of the interactions in the theory to be used will be done by obtaining them from electroweak theory, to

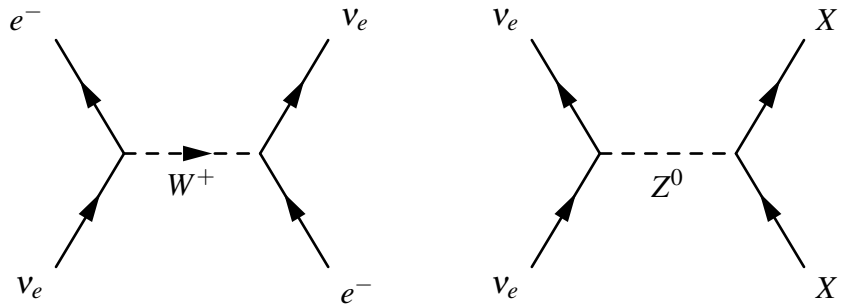

Figure 3.1: Feynman diagrams of coherent forward scattering processes through charged (left) and neutral (right) current. X represents an electron or a nucleon, and ν_α, any flavor of neutrino.

ensure a correct understanding of the phenomenon, and following the procedure in [2].

Specifically, the processes that will affect neutrinos in a medium are coherent scattering, where the interaction makes the other interacting particle recoils as a whole and remain in the same quantum state (Fig. (3.1)), and incoherent scattering, where the other interacting particle recoils as a whole, but changes its quantum state. The two processes as basically indistinguishable experimentally if only the recoil energy is observed [17]. However, the latter is a small fraction of the total scattering events, as the neutrino mean free path considering in normal matter can be demonstrated to be about 0.1 light years [2]. Thus, we can neglect this process.

3.1 Evolution equation

The number of events of coherent interactions will not be vanishingly small and they will affect the neutrino flavor states evolution, as they add an effective potential term to the energy. Let us recall the Schrödinger equation:

$$i\frac{d}{dx}\nu = \mathscr{H}\nu \tag{3.1}$$

For our case, $\mathscr{H}$ is the total Hamiltonian, and includes matter effects as:

$$\mathscr{H} = \mathscr{H}_0 + \mathscr{H}_I \tag{3.2}$$

where $\mathscr{H}_I|\nu_\alpha\rangle = V_\alpha|\nu_\alpha\rangle$. In Eq.(3.2), $\mathscr{H}_0$ represents the vacuum hamiltonian, related only to neutrino masses, and $\mathscr{H}_I$ represents the interaction with matter that is being added. V_α is the matter potential that will modify the energy the neutrino would have in vacuum, and the eigenvalue when applying $\mathscr{H}_I$ to neutrino flavor states. The expression for V_α can be found from the formulation of the interaction in electroweak theory. For the case of the charged current shown in Fig. (3.1), the effective Hamiltonian is:

$$\mathscr{H}^{CC}(x) = \frac{G_F}{\sqrt{2}}[\overline{\nu_e}(x)\gamma^\rho(1-\gamma^5)e(x)][\overline{e}(x)\gamma_\rho(1-\gamma^5)\nu_e(x)] \tag{3.3}$$

Now, we actually need to find $\overline{\mathscr{H}}^{CC}(x) = \langle\int\mathscr{H}^{CC}(x)dx\rangle$, averaged over the electron background. However, Eq.(3.3) cannot be inserted directly, as pointed out in [18]. The electrons in a medium have an energy distribution, described by the Fermi function: $f(E_e,T)$ ($\int f(E_e,T)dp_e = 1$), so we have to also integrate over it. At the same time, the polarization of the electrons is unknown, so we need to average over spin, h_e: $\frac{1}{2}\sum_{h_e}$. Thus:

$$\mathscr{H}'^{CC}(x) = \frac{1}{2}\sum_{h_e}\int\frac{G_F}{\sqrt{2}}[\overline{\nu_e}(x)\gamma^\rho(1-\gamma^5)e(x)][\overline{e}(x)\gamma_\rho(1-\gamma^5)\nu_e(x)]dp_e \tag{3.4}$$

To follow the calculations, we first need to keep in mind that a Fierz transfor-

mation allows us to rearrange the expression with:

$$[\overline{\nu_e}(x)\gamma^\rho(1-\gamma^5)e(x)][\overline{e}(x)\gamma_\rho(1-\gamma^5)\nu_e(x)] = [\overline{e}(x)\gamma^\rho(1-\gamma^5)e(x)][\overline{\nu_e}(x)\gamma_\rho(1-\gamma^5)\nu_e(x)] \tag{3.5}$$

We also need to remember the quantized fields:

$$e(x) = \frac{1}{\sqrt{2E_eV}} e^{-ip_e x} u_{h_e}(p_e) a_{h_e}(p_e) \tag{3.6}$$

$$\overline{e(x)} = \frac{1}{\sqrt{2E_eV}} e^{ip_e x} a^\dagger_{h_e}(p_e) \overline{u_{h_e}}(p_e), \tag{3.7}$$

where E_e is the electron energy and V is the volume in space, a and $a^\dagger$ are the annihilation and creation operators, and u and $\overline{u}$, the spinors for an electron spin h_e and momentum p_e. We then get:

$$\mathscr{H}'^{CC}(x) = \frac{1}{2}\sum_{h_e}\int \frac{G_F}{2\sqrt{2}E_eV}[N_{h_e}(p_e)\overline{u_{h_e}}(p_e)\gamma^\rho(1-\gamma^5)u_{h_e}(p_e)][\overline{\nu_e}(x)\gamma_\rho(1-\gamma^5)\nu_e(x)]dp_e, \tag{3.8}$$

where $N_{h_e}(p_e) = a^\dagger_{h_e}(p_e)a_{h_e}(p_e)$ is the number operator. Eq.(3.8) can actually be used to find $\overline{\mathscr{H}}^{CC}(x)$:

$$\overline{\mathscr{H}}^{CC}(x) = \langle \nu_e(p_\nu,h_\nu)e(p_e,h_e)| \int \mathscr{H}'^{CC}(x)dx |\nu_e(p_\nu,h_\nu)e(p_e,h_e)\rangle \tag{3.9}$$

For some final steps, we will need some other identities. First, we will consider

equal number of electrons with positive and negative spin:

$$N_{h_e}(p_e)\,|e(h+,p_e)\rangle = N_{h_e}(p_e)\,|e(h-,p_e)\rangle = VN_e(p_e)\,|e(h_e,p_e)\rangle \tag{3.10}$$

Notice that the number density of electrons, $N_e(p_e)$ still depends on the momentum. We will also need:

$$\sum_{h_e} \overline{u_{h_e}}(p_e)\gamma^\rho(1-\gamma^5)u_{h_e}(p_e) = 4P_e^\rho \tag{3.11}$$

$$\int f(E_e,T)N_e(p_e)\frac{\vec{\gamma}\cdot\vec{p}_e}{E_e(p_e)} = 0, \tag{3.12}$$

as the integrand is odd under $\vec{p}_e \to -\vec{p}_e$, and

$$\int f(E_e,T)N_e(p_e)dp_e = N_e, \tag{3.13}$$

where N_e is finally the number density of electrons in the medium. So, we finally arrive at:

$$\overline{\mathscr{H}}^{CC}(x) = V_{CC}\overline{\nu_{e,L}}(x)\gamma^0\nu_{e,L}(x) \tag{3.14}$$

where $V_{CC} = \sqrt{2}G_F N_e$. Similarly, the effective Hamiltonian for the neutral current interaction is:

$$\mathscr{H}^{NC}(x) = \frac{G_F}{\sqrt{2}}\sum_\alpha[\overline{\nu_\alpha}(x)\gamma^\rho(1-\gamma^5)\nu_\alpha(x)]\sum_f[\overline{f}(x)\gamma_\rho(g_v^f - g_A^f\gamma^5)f(x)] \tag{3.15}$$

By comparing with our previous equations, we arrive at the potential for neutral current $V_{NC}^f = \sqrt{2}G_F N^f g_V^f$ for each particle represented by f [2], where g_V^f are real dimensionless parameters for the couplings of the Z boson to fermions

[19]. The values of g_V^f are shown in the following table [2]:

Fermion	g_V^f
ν_l	$g_V^\nu = \frac{1}{2}$
l	$g_V^l = -\frac{1}{2} - 2s_W^2$
u,c,t	$g_V^U = \frac{1}{2} - \frac{4}{3}s_W^2$
d,s,b	$g_V^D = -\frac{1}{2} + \frac{2}{3}s_W^2$

Table 3.1: Values of g_V^f for fermions.

where $s_W^2 = \sin \vartheta_W{}^2$ and ϑ_W is the weak mixing angle. Also, for hadrons, such as protons and neutrons:

$$g_V^p = 2g_V^u + g_V^d, \quad g_V^n = g_V^u + 2g_V^d \tag{3.16}$$

The sums over neutrino flavors α and particles f appear because the interaction is not limited to only electrons and electron neutrinos. However, this also implies that the potentials produced by interactions with protons and electrons will cancel out, as their values for g_V^f are the same, but with opposite signs. Therefore, the potential will be reduced to that of the interaction between neutrinos and neutrons, and we arrive at:

$$V_{NC} = -\frac{1}{2}\sqrt{2}G_F N_n \tag{3.17}$$

Finally, the potentials can be summarized as [2]:

$$\overline{\mathscr{H}}_{eff}(x) = \sum_{\alpha=e,\mu,\tau} V_\alpha \overline{\nu_{\alpha,L}}(x)\gamma^0 \nu_{\alpha,L}(x) \tag{3.18}$$

$$V_\alpha = V_{CC}\delta_{\alpha e} + V_{NC} \tag{3.19}$$

We can now express the total Hamiltonian in matrix form, taking into account

that the eigenstates of $\mathscr{H}_0$ are the neutrino mass states, while the eigenstates of $\mathscr{H}_I$ are the flavor states. On top of that, we will express the $\mathscr{H}_0$ eigenvalues as the relativistic approximation for the energy, $E = p + \frac{m^2}{2E}$. Our total $\mathscr{H}$ then will be, in the flavor basis:

$$\mathscr{H} = U \begin{pmatrix} p + \frac{m_1^2}{2E} & 0 & 0 \\ 0 & p + \frac{m_2^2}{2E} & 0 \\ 0 & 0 & p + \frac{m_3^2}{2E} \end{pmatrix} U^\dagger + \begin{pmatrix} V_{CC} + V_{NC} & 0 & 0 \\ 0 & V_{NC} & 0 \\ 0 & 0 & V_{NC} \end{pmatrix} \tag{3.20}$$

The terms with V_{NC} in $\mathscr{H}_I$ will only add a global phase to any flavor state we will be evaluating, and so will the term $p + \frac{m_1^2}{2E}$ from $\mathscr{H}_0$. Then, we can take the terms out and finally obtain:

$$\mathscr{H} = \frac{1}{2E}(U\mathscr{M}^2 U^\dagger + A) \tag{3.21}$$

where U is the PMNS matrix and $\mathscr{M}^2$ and A are defined as [2]:

$$\mathscr{M}^2 = \begin{pmatrix} 0 & 0 & 0 \\ 0 & \Delta m_{21}^2 & 0 \\ 0 & 0 & \Delta m_{31}^2 \end{pmatrix} \tag{3.22}$$

$$A = \begin{pmatrix} A_{CC} & 0 & 0 \\ 0 & 0 & 0 \\ 0 & 0 & 0 \end{pmatrix} \tag{3.23}$$

with $A_{CC} \equiv 2EV_{CC} = 2\sqrt{2}EG_F N_e$.

3.1.1 Analytical solution of the two generation case

For two generation oscillations, for example, the new term in the Hamiltonian will modify the sole mixing angle considered in vacuum oscillations. With the mixing matrix in Eq.(2.3), the effective hamiltonian in the flavor basis can be expressed as:

$$\mathscr{H} = \begin{pmatrix} -\frac{\Delta m^2}{2E}\cos 2\theta + \sqrt{2}G_F N_e & \frac{\Delta m^2}{4E}\sin 2\theta \\ \frac{\Delta m^2}{4E}\sin 2\theta & 0 \end{pmatrix} \tag{3.24}$$

The diagonalization gives a matrix of the form:

$$\mathscr{H} = \begin{pmatrix} \lambda_+ & 0 \\ 0 & \lambda_- \end{pmatrix}, \tag{3.25}$$

and the eigenvalues:

$$\lambda_\pm = \frac{-A \pm \sqrt{A^2 + 4B^2}}{2}, \tag{3.26}$$

where

$$X = -\frac{\Delta m^2}{2E}\cos 2\theta + \sqrt{2}G_F N_e \qquad Y = \frac{\Delta m^2}{4E}\sin 2\theta \tag{3.27}$$

The corresponding eigenstates are:

$$|+\rangle = \frac{\lambda_+}{\sqrt{\lambda_+^2 + Y^2}}|\nu_\alpha\rangle + \frac{Y}{\sqrt{\lambda_+^2 + Y^2}}|\nu_\beta\rangle \tag{3.28}$$

$$|-\rangle = \frac{\lambda_-}{\sqrt{\lambda_-^2 + Y^2}} |\nu_\alpha\rangle + \frac{Y}{\sqrt{\lambda_-^2 + Y^2}} |\nu_\beta\rangle \tag{3.29}$$

and the probability of starting with a flavor ν_α and detecting ν_β gives:

$$P_{\nu_\alpha \to \nu_\beta} = \frac{4Y^2}{X^2 + 4Y^2} \sin^2\left(\sqrt{X^2 + 4Y^2}\frac{L}{2}\right) \tag{3.30}$$

Finally, this can be rearranged in the form of Eq.(2.8) as:

$$P_{\nu_\alpha \to \nu_\beta} = \sin^2 2\theta_M \sin^2\left(\frac{\Delta m_M^2}{4E} L\right), \tag{3.31}$$

where the new variables are defined as [2]:

$$\Delta m_M^2 = 2\sqrt{X^2 + 4Y^2} = \sqrt{(\Delta m^2 \cos 2\theta - Acc)^2 + (\Delta m^2 \sin 2\theta)^2} \tag{3.32}$$

$$\sin(2\theta_M) = \frac{4Y^2}{X^2 + 4Y^2} = \frac{\Delta m^2 \sin 2\theta}{\Delta m_M^2} \tag{3.33}$$

3.2 Mikheyev-Smirnov-Wolfenstein Effect

We have established that neutrino flavor conversion is a product of coherent mixtures of mass eigenstates, which will have different phases when evolving, and this relative phase will produce interference. We have also established that, when propagating in normal media, the hamiltonian for the neutrino flavors will depend on the effective potential due only to charged current interactions. The observed oscillation parameters then change according to Eq.(3.32) and (3.33). Notice that there will appear a resonance in the oscillation probability when Δm_M^2 reaches its minimum:

$$A_{CC} = \Delta m^2 \cos 2\theta \tag{3.34}$$

This potential will be given when the electron number density resonance density:

$$N_e^R = \frac{\Delta m^2 \cos 2\theta}{2\sqrt{2} E G_F} \tag{3.35}$$

The effective mixing angle then gives $\theta_m = \pi/4$. At this resonance, the initial flavor can completely disappear [2]. This is the Mikheyev, Smirnov, Wolfenstein (MSW) Effect and it evidences the difference between oscillations in vacuum and matter as follows.

For media with constant matter density, enhanced transitions are produced. As the new parameters for the probabilities will still be fixed with a certain value of N_e, their oscillatory behavior observed in vacuum remains [20]. However, the effective potential for normal matter is positive and the resonance density in Eq. (3.35) can only happen if $\theta < \pi/4$. Then, the probability is not symmetric if we change θ for $\pi/2 - \theta$, as it is in vacuum [2].

Chapter 4

Non-Standard Neutrino Interactions (NSI)

The phenomenon of neutrino oscillations is by itself proof of physics beyond the Standard Model. However, opens the possibility to consider several other hypotheses for describing nature. We will focus on the so-called Non-Standard Neutrino Interactions (NSI). These were first proposed by Wolfenstein as a mechanism to induce flavor changes for massless neutrinos from their interactions with matter, thus solving the solar neutrino problem [21]. While mass-induced neutrino oscillations explain the available data well and are considered as the "standard" solution for the changes in flavor, sub-leading effects from New Physics may still be present and not contradict the current observations, as studied in, for example, [22] and [23].

4.1 Motivation

In his original work, Wolfenstein evaluated a simple model with two massless neutrino flavors, a and b, defined by the standard charged current. The coherent forward scattering process was still considered, although the neutrino neutral

current in the model included both diagonal and off-diagonal terms, and was written as:

$$\begin{aligned} L_\lambda = \cos^2\alpha[\bar{\nu}_a\gamma_\lambda(1+\gamma_5)\nu_a + \bar{\nu}_b\gamma_\lambda(1+\gamma_5)\nu_b] \\ + \sin^2\alpha[\bar{\nu}_a\gamma_\lambda(1+\gamma_5)\nu_b + \bar{\nu}_b\gamma_\lambda(1+\gamma_5)\nu_a] \end{aligned} \tag{4.1}$$

Following this approach, the passage of neutrinos from the core to the surface of the sun was studied. Even in the extreme case where the neutral current scattering always changes the neutrino flavor, $\sin^2\alpha = 1$, the mechanism turned out to only partially account for the observed deficit of solar neutrinos. Furthermore, $\sin^2\alpha$ cannot be equal to 1, as it is in disagreement with the constraints given by hadron-lepton universality [21]. Even if this is not the solution for neutrino flavor change, it cannot be totally discarded.

4.2 Theoretical framework

Although the goal of this work is a model-independent study of the phenomenon, it is relevant to mention how theoretical frameworks may support the existence of Non-Standard Interactions. In fact, if neutrino oscillations call for non-zero neutrino masses, we need to consider the scenarios to obtain them, and see-saw suppression offers a way not only induce the masses, but to have them be small. Adding, for instance, $SU(2)_L$ singlets leads to an extended leptonic mixing matrix, and all interaction states become a superposition of light and heavy mass states. Thus, the neutral current operator must be projected onto the light

mass states subspace so that it represents the interaction at low energies. This is equivalent to simply considering U_{PMNS}, between the three neutrino flavors and light mass states, but it would be a part of a larger matrix now. While the extended mixing matrix is unitary, the *submatrix* U_{PMNS} is not, and off-diagonal matrix elements for the effective neutral current operator are found [24]. A more formal derivation of this type of new interactions starting from neutrino mass generation can be found in [25].

Non-Standard Interaction processes include $\nu_\alpha f \to \nu_\beta f$, for $\alpha \neq \beta$, and $\nu_\alpha f \to \nu_\alpha f$, called Flavor Changing Neutral Currents (FCNC) and Flavor Diagonal Neutral Currents (FDNC), respectively. The latter has the exact same form as the standard process, but the possibility of being non-universal is considered, so it would not add a global phase to the neutrino states. Although the new interactions can also involve charged currents and, more specifically, the Lagrange density for charged NSI with electrons can be transformed to be mathematically equivalent to neutral current NSI, these are strongly constrained in comparison to the neutral current processes. Thus, when studying neutrino propagation through matter, only neutral currents are considered.

Posed from an Effective Field Theory, as in Wolfenstein's original proposal, the new interactions with a target fermion f that causes the mixing ν_α and ν_β are described as:

$$\mathscr{L} = -2\sqrt{2}G_F \sum_P \varepsilon_{\alpha\beta}^{f,P} (\bar{\nu}_\alpha \gamma^\mu P_L \nu_\beta)(\bar{f}\gamma_\mu P f), \tag{4.2}$$

where G_F is the Fermi constant. P represents $\{P_R, P_L\}$, as the interaction with

both the left and right chirality parts of the fermion are included, each quantified by the ε coefficients. This particular structure for the Lagrange density allows the representation of the coherent contribution of NSI to Standard Model processes. Eq. (4.2) can also be written in terms of the vector and axial components of the interactions [26], as:

$$\mathscr{L} = -\sqrt{2}G_F(\bar{\nu}_\alpha\gamma^\mu P_L\nu_\beta)[\bar{f}\gamma_\mu(\varepsilon^f_{\alpha\beta V} + \varepsilon^f_{\alpha\beta A}\gamma^5)f], \tag{4.3}$$

Let us recall Eq. (3.15), which is completely analogous to Eq. (4.3). The resulting matter potential will once again have the vector part as the only surviving term, as it is the case for chiral interactions in general, and give $V^f_{\alpha\beta} = \sqrt{2}G_F N_f \varepsilon^f_{\alpha\beta V}$.

Now, for the overall non-standard matter potential in normal matter, we will also need to sum over fermions $f \in \{u,d,e\}$. The total Hamiltonian will then still be Eq. (3.21), except that the A matrix will now be:

$$A = A_{CC}\begin{pmatrix} 1+\varepsilon_{ee} & \varepsilon_{e\mu} & \varepsilon_{e\tau} \\ \varepsilon_{\mu e} & \varepsilon_{\mu\mu} & \varepsilon_{\mu\tau} \\ \varepsilon_{\tau e} & \varepsilon_{\tau\mu} & \varepsilon_{\tau\tau} \end{pmatrix}, \tag{4.4}$$

where each $\varepsilon_{\alpha\beta} = \sum_{f=e,u,d}\varepsilon^f_{\alpha\beta V}\frac{N_f}{N_e}$. Each diagonal ε is a real number, while every off-diagonal element is $\varepsilon_{\alpha\beta} = |\varepsilon_{\alpha\beta}|e^{\phi_{\alpha\beta}}$. Moreover, $\varepsilon_{\beta\alpha} = \varepsilon^*_{\alpha\beta}$ to ensure the hermiticity of the Hamiltonian.

A useful expression for the appearance channel ($\nu_\mu \to \nu_e$) probability can be found by making an expansion in some oscillation parameters. Particularly, if

we consider $\sin\theta_{13}$ and the non-diagonal ε parameters to be small, as done in [27], we obtain:

$$\begin{aligned}
P_{\nu_\mu\to\nu_e} &= x^2f^2 + 2xyfg\cos(\Delta+\delta_{CP}) + y^2g^2 + 4\hat{A}\varepsilon_{e\mu}\{xf[s_{23}^2 f\cos(\phi_{e\mu}+\delta_{CP}) \\
&+ c_{23}^2 g\cos(\Delta+\delta_{CP}+\phi_{e\mu})] + yg[c_{23}^2 g\cos\phi_{e\mu} + s_{23}^2 f\cos(\Delta-\phi_{e\mu})]\} \\
&+ 4\hat{A}\varepsilon_{e\tau}s_{23}c_{23}\{xf[f\cos(\phi_{e\tau}+\delta_{CP}) - g\cos(\Delta+\delta_{CP}+\phi_{e\tau})] \\
&- yg[g\cos\phi_{e\tau} - f\cos(\Delta-\phi_{e\tau})]\} + 4\hat{A}^2g^2c_{23}^2|c_{23}\varepsilon_{e\mu} - s_{23}\varepsilon_{e\tau}|^2 \\
&+ 4\hat{A}^2f^2s_{23}^2|s_{23}\varepsilon_{e\mu} + c_{23}\varepsilon_{e\tau}|^2 + 8\hat{A}^2fgs_{23}c_{23}\{c_{23}\cos\Delta[s_{23}(\varepsilon_{e\mu}^2 - \varepsilon_{e\tau}^2) \\
&+ 2c_{23}\varepsilon_{e\mu}\varepsilon_{e\tau}\cos(\phi_{e\mu}-\phi_{e\tau})] - \varepsilon_{e\mu}\varepsilon_{e\tau}\cos(\Delta-\phi_{e\mu}+\phi_{e\tau})\} \\
&+ O(s_{13}^2\varepsilon, s_{13}\varepsilon^2, \varepsilon^3),
\end{aligned} \tag{4.5}$$

where

$$\begin{aligned}
&x = 2s_{13}s_{23}, \quad y = 2rs_{12}c_{12}c_{23}, \quad r = |\Delta m_{21}^2/\Delta m_{31}^2|, \quad \hat{A} = \left|\frac{A}{\Delta m_{31}^2}\right|, \\
&f, \bar{f} = \frac{\sin[\Delta(1\mp\hat{A}(1+\varepsilon_{ee}))]}{(1\mp\hat{A}(1+\varepsilon_{ee}))}, \quad g = \frac{\sin(\hat{A}(1+\varepsilon_{ee})\Delta)}{\hat{A}(1+\varepsilon_{ee})}, \\
&\Delta = \left|\frac{\Delta m_{31}^2 L}{4E}\right|, \quad s_{ij} = \sin\theta_{ij}, \quad c_{ij} = \cos\theta_{ij}
\end{aligned} \tag{4.6}$$

When considering antineutrinos, the probability is found using $\bar{f}$, $\hat{A}\to-\hat{A}$, $\delta_{CP}\to-\delta_{CP}$ and $\phi_{\alpha\beta}\to-\phi_{\alpha\beta}$.

4.3 Other Non-Standard Interactions

As previously mentioned, the new interactions do not have to necessarily be the result of neutral currents. They can also be charged current processes, and

change the interacting lepton flavor. Although non-standard charged current interactions do not have a notorious effect in neutrino propagation, they may in fact play a larger role in neutrino production and detection, considering two aspects:

- Neutrino production and detection are based on charged current interactions, so they can distinguish among neutrino flavors.
- While current data analyses seem to point towards charged current NSI parameters that are much better constrained than neutral current ones, there is no fundamental reason to consider them to be vanishingly small [28]. In fact, as we reach higher energies and better precision in experiments, the effects of charged currents may very well become visible.

Charged current non-standard interactions are expressed as:

$$\mathscr{L} = -2\sqrt{2}G_F \sum_P \varepsilon_{\alpha\beta}^{ff',P} (\bar{\nu}_\alpha \gamma^\mu P_L l_\beta)(\bar{f}\gamma_\mu P f'), \tag{4.7}$$

where $\alpha \neq \beta$. The corresponding ε parameters, of course, depend on the specific fermions involved in the process.

4.3.1 NSI in neutrino production and detection

As pointed out in [29], if the new interactions are present, these could allow, for example, a muon neutrino to produce an electron neutrino in the detector, which would lead us to a misinterpretation of the flavor change as a contribution to the oscillation observations. The theoretical description for this considers that

flavor states in both neutrino source and detector can be expressed in the same fashion as Eq. (2.1), but with different mixing matrices:

$$|\nu^s_\alpha\rangle = \sum_i U^s_{\alpha i} |\nu_i\rangle \,, \tag{4.8}$$

$$|\nu^d_\alpha\rangle = \sum_i U^d_{\alpha i} |\nu_i\rangle \,, \tag{4.9}$$

where the indices s and d represent source and detector respectively, and once again Latin letters denote mass eigenstates. Then, having no matter effects and only neutrino flavor ν^s_α in the source, a neutrino flavor ν^d_β could be found in the detector with probability [29]:

$$\begin{aligned} P_{\beta\alpha}(t) = |\langle \nu^d_\beta | \nu^s_\alpha \rangle (t)|^2 &= \left| \sum_{ij} \langle \nu_j | U^{d\dagger}_{j\beta} e^{-iE_i t} U^s_{\alpha i} | \nu_i \rangle \right|^2 \\ &= \sum_{ij} |U^s_{\alpha i} U^{s*}_{\alpha j} U^{d*}_{\beta i} U^d_{\beta j}| \cos[(E_i - E_j)t - \arg(U^s_{\alpha i} U^{s*}_{\alpha j} U^{d*}_{i\beta} U^d_{j\beta})] \end{aligned} \tag{4.10}$$

From Eq. (4.10), an effect that does not depend on the propagation can already be seen. Let us recall that the existence of NSI in no way implies that the three neutrino flavors, as defined by the standard charged current, have changed, but rather that the production and detection processes may have eigenstates different to them. So we would have a neutrino mass basis, a neutrino flavor basis and another two bases, whose eigenstates are superpositions of flavor states. These states can therefore be parametrized as [30]:

$$|\nu^s_\alpha\rangle = |\nu_\alpha\rangle + \sum_{\gamma=e,\mu,\tau} \varepsilon^s_{\alpha\gamma} |\nu_\gamma\rangle \tag{4.11}$$

$$\langle \nu_\beta^d| = \langle \nu_\beta| + \sum_{\gamma=e,\mu,\tau} \varepsilon_{\gamma\beta}^d \langle \nu_\gamma| \tag{4.12}$$

The parameter matrices ε^s and ε^d are arbitrary and non-unitary in general, as they correspond to the previously defined charged current NSI parameters and they depend on the physical processes for production and detection [31]. Thus, the source and detector states are no longer orthonormal. New normalization factors need to be introduced in the states so that the transition probabilities can actually be defined [32]:

$$|\nu_\alpha^s\rangle = \frac{1}{N_\alpha^s}\left(|\nu_\alpha\rangle + \sum_{\gamma=e,\mu,\tau} \varepsilon_{\alpha\gamma}^s |\nu_\gamma\rangle\right) \tag{4.13}$$

$$\langle \nu_\beta^d| = \frac{1}{N_\beta^d}\left(\langle \nu_\beta| + \sum_{\gamma=e,\mu,\tau} \varepsilon_{\gamma\beta}^d \langle \nu_\gamma|\right), \tag{4.14}$$

where the normalization factors can be written as:

$$N_\alpha^s = \sqrt{[(1+\varepsilon^s)(1+\varepsilon^{s\dagger})]_{\alpha\alpha}} \tag{4.15}$$

$$N_\beta^d = \sqrt{[(1+\varepsilon^{d\dagger})(1+\varepsilon^d)]_{\beta\beta}} \tag{4.16}$$

However, the source and detector bases are still not orthogonal, and, as mentioned in [32] and [31], this implies that the new normalization will also affect calculations for neutrino fluxes and cross-sections. This can be handled in different ways:

- When calculating an estimate for the number of events in experiments

simulations, normalization terms cancel out once fluxes, probabilities and cross-sections are all corrected. Therefore, the states as defined in Eq. (4.11) and (4.12) are used as effective flavor states for obtaining effective transition probabilities [32].

- When using a near detector to directly measure the neutrino flux in an experiment, the normalization factors must be included for the transition probabilities and cross-sections [31].

4.3.2 Zero-distance effect

Considering Eq. (4.11) and (4.12) as our flavor states, and once again, no matter effects, the transition probability gives [33]:

$$\begin{aligned} P_{\beta\alpha}(L) = |\langle \nu^d_\beta | \nu^s_\alpha \rangle (L)|^2 &= \left| \sum_{\gamma\delta i} (1+\varepsilon^d)_{\gamma\beta} (1+\varepsilon^s)_{\alpha\delta} U_{\delta i} U^*_{\gamma i} e^{-i\frac{m_i^2 L}{2E}} \right|^2 \\ &= \sum_{ij} \mathscr{J}^{i}_{\alpha\beta} \mathscr{J}^{j*}_{\alpha\beta} - 4 \sum_{i>j} \mathrm{Re}(\mathscr{J}^{i}_{\alpha\beta} \mathscr{J}^{j*}_{\alpha\beta}) \sin^2\left(\frac{\Delta m^2_{ij} L}{4E}\right) \\ &+ 2 \sum_{i>j} \mathrm{Im}(\mathscr{J}^{i}_{\alpha\beta} \mathscr{J}^{j*}_{\alpha\beta}) \sin\left(\frac{\Delta m^2_{ij} L}{2E}\right), \end{aligned} \tag{4.17}$$

where

$$\mathscr{J}^{i}_{\alpha\beta} = U^*_{\alpha i} U_{\beta i} + \sum_\gamma \varepsilon^s_{\alpha\gamma} U^*_{\gamma i} U_{\beta i} + \sum_\gamma \varepsilon^d_{\gamma\beta} U^*_{\alpha i} U_{\gamma i} + \sum_{\gamma\delta} \varepsilon^s_{\alpha\gamma} \varepsilon^d_{\delta\beta} U^*_{\gamma i} U_{\delta i} \tag{4.18}$$

The aforementioned effect of production and detection NSI which does not depend on the propagation can be seen more clearly. If $L = 0$, the first term in

Eq. (4.17) may still remain and is, in general, different from zero (or one). This is the *zero-distance effect* [33]: There is a flavor transition term that is constant, independent of the distance and should not be considered a contribution to neutrino oscillations. This effect could be the reason behind the observation of some signals at short baseline neutrino experiments [34].

4.4 NSI Constraints

4.4.1 Charged Current NSI

Given that large charged-current NSI parameters are difficult to induce in specific models, to correctly estimate the possible effects of these processes in experiments, model-independent constraints must be found. Bounds for specific NSI parameters have been found from the review of well-known experimental measurements and the processes involved.

The work in [28] derives the constraints as follows. It is noted that the Fermi constant, G_F, is most precisely determined from the muon decay rate. However, the muon decay process, $\mu^- \to e^- + \bar{\nu}_e + \nu_\mu$, could be affected by charged-current NSI and measurements could correspond to another constant $G_\mu = G_F f$, where $f = f\left(\varepsilon_{e\mu}^{\mu eL}, \sum_{\alpha\beta P} |\varepsilon_{\alpha\beta}^{\mu eP}|^2\right)$ is a function that carries the information about NSI coherent contribution to standard interactions and overall incoherent contributions. On the other hand, the Standard Model predicts a relation between the Fermi constant and the masses of the W and Z bosons [19]. These are determined from kinematic measurements, so there is no new interaction effects, and a comparison of G_μ and G_F gives bounds for $\varepsilon_{e\mu}^{\mu eL}$ and $|\varepsilon_{\alpha\beta}^{\mu eP}|$.

Similarly, the test of the CKM matrix unitarity is considered. This test is done through the determination of V_{ud} and V_{us} from beta and Kaon decay rates, which are predicted using G_F. From the previous discussion, if G_μ is used instead, the actual measured quantities are $|V_{ux}^M|^2 \equiv \frac{|V_{ux}|^2}{f^2}$, assuming that leptonic NSI is the dominating effect. By assuming CKM unitarity, bounds on the parameters can be found.

Comparisons of the amplitudes of π and τ decays are also evaluated for constraining the parameters, and the results of short baseline neutrino experiments are taken into account to support study the zero-distance effect. For this work, we consider the results in [28] as:

$$|\varepsilon_{\alpha\beta}^{s/d}| < \begin{pmatrix} 0.041 & 0.030 & 0.041 \\ 0.026 & 0.078 & 0.030 \\ 0.12 & 0.030 & 0.13 \end{pmatrix} \tag{4.19}$$

This approach takes into account the weaker between the bounds found from each specific process.

4.4.2 Neutral Current NSI

Analyses of the current available data from neutrino experiments, namely solar, atmospheric, reactor and long baseline neutrino experiments can point toward an agreement between the behavior of nature and a specific theoretical model. The obtained data sets should show a preference for certain theoretical framework, as the best possible fits for the data with different NSI couplings will give the constraints [26]. For example, it has been found that a small NSI effect

such as $\varepsilon_{ee}^{dV} \simeq 0.3$ gives a better fit of the data than the standard oscillation solution at 2σ [35]. Furthermore, it has been pointed out that this could be the key to solving tensions between the types of experiments, as the impact of matter potentials is different of each one of them.

While NSI constraints can be considered as the interaction of neutrinos with single quarks or leptons and constraints have been found for those cases (See [35]), we are interested in the total effect in the propagation of neutrino flavors in a medium, as presented in Eq. (4.4). From the global analysis in [36], we obtain for the moduli of NSI parameters:

$$|\varepsilon_{\alpha\beta}| < \begin{pmatrix} 2.45 & 0.19 & 0.44 \\ 0.19 & 1.6365 & 0.03509 \\ 0.44 & 0.03509 & 1.6481 \end{pmatrix} \tag{4.20}$$

and the corresponding phases can take values in $[-180^\circ, 180^\circ)$.

These constraints are good approximations, although not precise values, as we consider the positive bounds and consider all parameters independent. However, they give a general idea of the possible scenarios that could arise when studying the new interactions.

4.5 Effects of NSI in propagation

4.5.1 Impact on the effective mass

Let us review neutrino oscillations in matter for two generations, but modifying the matter potential to include Eq. (4.4). The effective hamiltonian in Eq. (3.24)

will now become:

$$\mathscr{H} = \begin{pmatrix} -\frac{\Delta m^2}{2E}\cos 2\theta + \sqrt{2}G_F N_e(1+\varepsilon_{ee}-\varepsilon_{\alpha\alpha}) & \frac{\Delta m^2}{4E}\sin 2\theta + \sqrt{2}G_F N_e \varepsilon_{e\alpha} \\ \frac{\Delta m^2}{4E}\sin 2\theta + \sqrt{2}G_F N_e \varepsilon_{e\alpha} & 0 \end{pmatrix} \tag{4.21}$$

The form of the matrix remains the same as in the standard interaction case and the transition probability will still be Eq. (3.31), but the quantities in Eq. (3.27), (3.32) and (3.33) will become:

$$A = -\frac{\Delta m^2}{2E}\cos 2\theta + \sqrt{2}G_F N_e(1+\varepsilon_{ee}-\varepsilon_{\alpha\alpha}) \tag{4.22}$$

$$B = \frac{\Delta m^2}{4E}\sin 2\theta + \sqrt{2}G_F N_e \varepsilon_{e\alpha} \tag{4.23}$$

$$\Delta m^2_M = \sqrt{(\Delta m^2 \cos 2\theta - A_{CC}(1+\varepsilon_{ee}-\varepsilon_{\alpha\alpha}))^2 + (\Delta m^2 \sin 2\theta + 2A_{CC}\varepsilon_{e\alpha})^2} \tag{4.24}$$

$$\sin(2\theta_M) = \frac{\Delta m^2 \sin 2\theta + 2A_{CC}\varepsilon_{\varepsilon_{e\alpha}}}{\Delta m^2_M} \tag{4.25}$$

Thus, the presence of NSI will change the mixing parameters. Furthermore, as noted in [37], this exact mechanism can cause for a misinterpretation of the measurements as a CPT violating phenomenon, contradicting our complete description of nature. From Eq. (4.24) and (4.25), we have for neutrinos:

$$\Delta m^2_M \sin(2\theta_M) = \Delta m^2 \sin 2\theta + 2A_{CC}\varepsilon_{\varepsilon_{e\alpha}} \tag{4.26}$$

$$\Delta m^2_M \cos(2\theta_M) = \Delta m^2 \cos 2\theta - A_{CC}(1 + \varepsilon_{ee} - \varepsilon_{\alpha\alpha}) \tag{4.27}$$

On the other hand, for antineutrinos, the matter potential must be of the opposite sign. So, assuming the NSI parameters to be real, we have:

$$\Delta m^2_M \sin(2\theta_M) = \Delta m^2 \sin 2\theta - 2Acc\varepsilon_{\varepsilon_{e\alpha}} \tag{4.28}$$

$$\Delta m^2_M \cos(2\theta_M) = \Delta m^2 \cos 2\theta + Acc(1 + \varepsilon_{ee} - \varepsilon_{\alpha\alpha}) \tag{4.29}$$

If we assume the vacuum mixing angle, θ, to be the same for both neutrinos and antineutrinos, we can obtain a simple expression for the difference between effective mixing angles for neutrinos and antineutrinos, thus could lead to a supposed CPT violation. In [37], it is also noted that T2K has reported such a difference. By using their reported values, they were able to perform a fit for the relevant NSI parameter and effectively reconstruct the CPT violation signal. This offers then an alternative solution rather than question the whole paradigm.

4.5.2 Degeneracies

While neutrino experiments are improved, reaching higher energies and more precise measurements, three of the six standard oscillation parameters remain undefined. Given the fact that several sets of parameters can give the same neutrino oscillation probability, rather than having definite values for them, there are several possible degenerate solutions, and they can be summarized as fol-

lows [38]:

1. The neutrino masses could follow the so-called normal hierarchy (NH), given $\Delta m^2_{31} > 0$, or inverted hierarchy (IH), given $\Delta m^2_{31} < 0$.

2. The θ_{23} mixing angle may be larger than 45°and belong to a higher octant (HO), or smaller than 45°and belong to a lower octant (LO).

3. δ_{CP} can still take any values between -180°and 180°, as CP-violation can be observed in long-baseline experiments, which also include matter effects and could lead to fake CP-violating signals [39].

These degeneracies remain when considering the Non-Standard Interactions. Furthermore, they can be enhanced by the presence of the new interactions, as evidenced by the study of the framework through perturbation theory [40]. Additionally, if NSI are present, then not only are there more parameters to constrain, but new degeneracies are found. Consider, for example, the solar mixing angle, θ_{12}: The Large Mixing Angle (LMA) solution, which includes both θ_{12} and Δm^2_{12}, has been considered the correct one, as solar neutrino observations agree with its predictions [41]. However, the data was analyzed in a framework including Non-Standard Interactions in [42] and gave way to the LMA-D solution, where an additional value of θ_{12} is obtained for the same value of Δm^2_{12}.

Moreover, degeneracies involving the NSI parameters arise when fitting data. As reported in [43], there appear two relevant degeneracies between standard and non-standard parameters. One degeneracy appears in the $\varepsilon_{\mu\mu}$ - θ_{23} plane, due to the dependence of the disappearance probability ($P_{\nu_\mu \to \nu_\mu}$) on both those

quantities. This may affect the expected precision when measuring θ_{23}. Another degeneracy is also found between δ_{CP} and the parameters ε_{ee} and $\varepsilon_{\tau e}$. How the presence of Non-Standard Interactions may affect observations of δ_{CP} will be described in more detail in the following section.

4.5.3 Misleading CP-violation signals

As mentioned before, long-baseline experiments may represent a good option to determine the CP-violating phase. A measurement of the CP-asymmetry can be defined as [44]:

$$A_{CP}(\delta_{CP}) = \frac{P_{\nu_\mu \nu_e}(\delta_{CP}) - P_{\bar{\nu}_\mu \bar{\nu}_e}(\delta_{CP})}{P_{\nu_\mu \nu_e}(\delta_{CP}) + P_{\bar{\nu}_\mu \bar{\nu}_e}(\delta_{CP})} \tag{4.30}$$

$$A_{CP}(\delta_{CP}) \approx \frac{\cos\theta_{23}\sin 2\theta_{12}\sin\delta_{CP}}{\sin\theta_{23}\sin\theta_{13}}\left(\frac{\Delta m^2_{21} L}{4E}\right) + \text{matter effects}, \tag{4.31}$$

where Eq. (4.30) is the general definiton, and Eq. (4.31) is a leading-order approximation of the first line for standard oscillations. So, rather than actually measuring the CP-violating phase, long baseline experiments can demonstrate CP-volation in general. The source of it is, however, unknown: whether it is a property of neutrinos, a result of matter effects or, if they are present, interference with the CP-violating phases of NSI parameters cannot be deduced from Eq. (4.30). Long baseline experiments then face the challenge of distinguishing

real from fake CP-violation signals.

For instance, recent results from NOvA and T2K experiments show a discrepancy in their measured values for δ_{CP}. Non-Standard Interactions are found to be a possible solution for this tension in [45] and [46]. It is noted that T2K has a baseline of 295 km and reaches its first oscillation maximum at $E \approx 0.6$ GeV and NOvA has a baseline of 810 km, with the first maximum at $E \approx 1.6$ GeV. The quantity $v = A_{CC}/\Delta m^2_{31}$ is then defined to measure each experiment's sensitivity to matter effects, giving close to 0.14 and 0.05 for NOvA and T2K respectively. Thus, NOvA is found to be more sensitive to NSI and it is argued that δ_{CP} measured at T2K is closer to its true value, while NOvA includes corrections from NSI according to:

$$\delta_{NOvA} \approx \delta_{T2K} + \phi_{e\beta}, \tag{4.32}$$

where $\beta = \mu, \tau$ [45].

A thorough study of the impact of NSI on CP-violation signals was done in [47]. By taking only one non-zero NSI parameter at a time to evaluate the effect of the new interactions, the research estimates the change in the oscillation probabilities thanks to either the modulus or the phase of a single parameter. The patterns are found to include contributions from New Physics and therefore lead to a wrong measurement of δ_{CP}. The effect that may be found on the oscillation probabilities will be shown explicitly in the following chapter.

Chapter 5

Analysis and Results

After solving the Schrödinger equation for the evolution of neutrino flavor states, the probabilities for flavor transitions can be obtained. For this work, a code for solving the equation numerically has been developed. It takes into account matter effects and a medium with constant density. An already existent package for neutrino experiments (GLoBES) has also been used, for comparing the solutions.

While neutrino oscillations have been extensively studied and packages for solving the differential equation are available, we considered the development of our own code to be an important first step. Being able to directly manage all parameters allows testing the sensitivity of the probabilities to them and achieving good control of the values. Furthermore, the effects of New Physics were introduced in the neutrino experiment simulation package (GLoBES). After the modifications, the new results were verified with the use of our code.

5.1 Developed code

The code for finding the numerical solution for the Schrödinger equation from Chapter 3 was developed using Python. The neutrino flavor states were defined as vectors with two or three complex components each, and the effective hamiltonians, as 2x2 or 3x3 matrices with complex elements, for oscillations in two or three generations respectively. Hermiticity of the hamiltonian is imposed by construction of the matrices. The method for solving the initial value problem was implicit, as our "vector components" are not independent. A function (solve_ivp) that contains Backward Differentiation Formulas (BDF), already implemented in the SciPy library [48], was used. Several relative and absolute tolerances were tried out as conditions for convergence of the solution, with different orders of magnitude (the relative error manages the number of correct digits in the result).

The results obtained with our code were verified, for the two-generation scenario, with the analytical formulas for both Standard and Non-Standard Interactions with matter, while the three-generation scenario was validated with the use of the package described in the following section, for only Standard interactions. Results for Non-Standard Interactions were compared to previous studies and were, in turn, used for a correct modification of the simulation software.

The values used throughout this work for the standard oscillation parameters for the Hamiltonian term, H_0, were the latest best-fit updates in NU-fit [49], and are shown in Table 5.1. The values for δ_{CP} will be stated for each example. The fraction of electrons in normal matter is taken to be ~ 0.494.

	Normal Hierarchy	Inverted Hierarchy
$\sin^2\theta_{12}$	0.304 ± 0.013	0.304 ± 0.013
$\sin^2\theta_{23}$	0.570 ± 0.024	0.575 ± 0.021
$\sin^2\theta_{13}$	0.02221 ± 0.00068	0.02240 ± 0.00062
$\Delta m^2_{21}/eV^2$	$(7.42 \pm 0.21) \times 10^{-5}$	$(7.42 \pm 0.21) \times 10^{-5}$
$\Delta m^2_{31}/eV^2$	$(2.514 \pm 0.028) \times 10^{-3}$	$(-2.497 \pm 0.028) \times 10^{-3}$

Table 5.1: Best-fit values for the standard oscillation parameters

5.2 General Long Baseline Experiment Simulator — GLoBES

GLoBES is a simulation software package for short and long baseline neutrino oscillation experiments [50]. It allows the description of experiments through a newly-defined language (AEDL), and processing the simulated data for fitting oscillation parameters. While the main purpose of GLoBES is the calculation of χ^2 and its projections onto certain subspaces of parameters, low-level information such as oscillation probabilities and event rates for specific experiments can also be read. For calculating the oscillation probabilities, the software takes a set of input data, including the initial and detected neutrino flavors, matter density and baseline, and applies a diagonalization algorithm for solving the Schrödinger equation.

An AEDL file describes an experiment by including its matter profile, baseline, detector cross-sections and efficiencies, and beam characteristics. It also defines the channels (processes to take place) and rules (one or more channels that may contribute to either neutrino appearance or disappearance). Thus, a specific experiment can also be passed as an argument for the calculation of

probabilities and event rates and spectra are obtained. Details on the functions and commands can be found in [51].

5.2.1 Modifying GLoBES

GLoBES does include a set of functions to allow the simulation of New Physics scenarios. This can be done by registering a probability engine and/or a probability matrix. The former allows for the modification of the hamiltonian only and, therefore, the evolution of the flavor states. The latter allows for the direct modification of probabilities, and it is useful for damping effects that result, for example, from the loss of coherence of neutrino wave packets. As Non-Standard Interactions are a hamiltonian level effect, their introduction involves the definition of a new probability engine rather than a new probability matrix (see [50]).

The default probability engine in the package includes six parameters and the standard oscillation hamiltonian, so for NSI to be described, nine new parameters must be described and the new probability engine must be registered with fifteen parameters. The hamiltonian in the probability engine file also has to be modified, to correspond to Eq.(4.4). Note we ensure the hermiticity of the new hamiltonian in this definition.

Finally, the entire program will use fifteen-parameter vectors at all times. While there are functions in GLoBES that allow setting parameter values with only one command, these work for the six standard oscillation parameters. Establishing the values for the non-standard parameters must be done one by one.

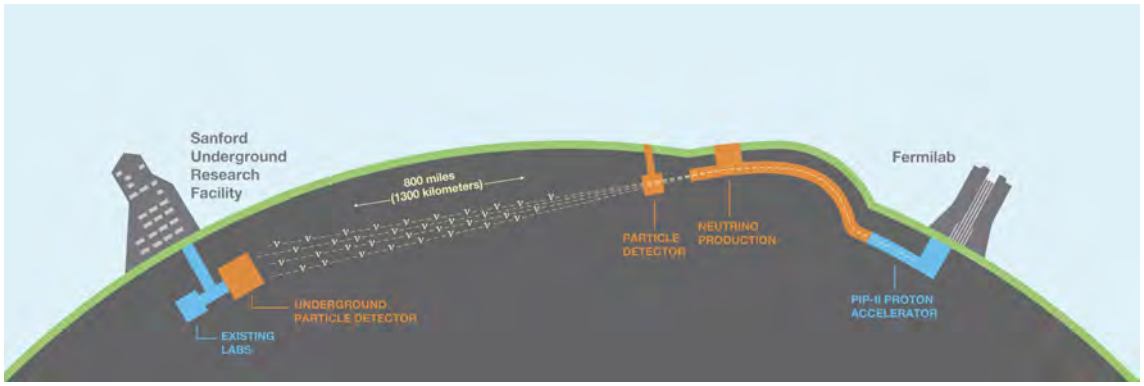

Figure 5.1: Deep Underground Neutrino Experiment: Neutrino beam path from production to far detector. Credit: Fermilab.

5.3 About DUNE experiment

The Deep Underground Neutrino Experiment (DUNE) is an international long baseline neutrino experiment that is currently in development. It was designed to continue the study of neutrino properties, with a high-intensity neutrino beam and high-precision measurements. Hosted by Fermilab, DUNE consists of a high-performance near detector on site and a massive liquid argon time-projection chamber far detector at the Sandford Underground Research Facility, giving way to a 1300 km baseline [52]. The path followed by the neutrino beam is sketched in Fig. 5.1.

More specifically, the design of the experiment aims to allow the determination of the CP-violating phase, δ_{CP}, the neutrino mass hierarchy and the octant of the θ_{23} mixing angle. Furthermore, it will also allow the exploration of Beyond Standard Model phenomena. As shown in [53], an experiment's discovery sensitivity to Non-Standard Interactions depends on the baseline length, making DUNE particularly relevant to study them.

Thus, the effects of NSI in this work will be considered in the context of DUNE.

For probability plots, both in our developed code an GLoBES, it is enough to know the baseline and matter density used in the experiment. The latter is obtained from the AEDL files provided by the DUNE collaboration [54], where the earth profile is considered to be a layer of about 1.5 km of depth and constant matter density, calculated using the Preliminary Earth Model [55].

5.4 Results

The plots included in this section aim to, rather than give fit values or numerical results, demonstrate the possible impact of Non-Standard Interactions on neutrino oscillation probabilities and the measurements of some of the parameters. For evaluating NSI in propagation in matter, the context of DUNE is used, meaning a baseline of 1300 km and matter density of 2.95 g/cm^3. Production and detection NSI are also considered separately, as the near detector at DUNE should keep fluxes controlled and therefore reduce the effect of charged-current new interactions.

5.4.1 NSI in neutrino production and detection

For this analysis, we use $\delta_{CP} = 0$, normal mass hierarchy, and the upper bounds for source and detector NSI values suggested in [56], which allow us to enhance the interactions, according to current data, but not break the constraints in section 4.4.1:

$$|\varepsilon_{\mu e}^{s/d}| < 0.0046, \quad |\varepsilon_{\mu\tau}^{s/d}| < 0.0018 \tag{5.1}$$

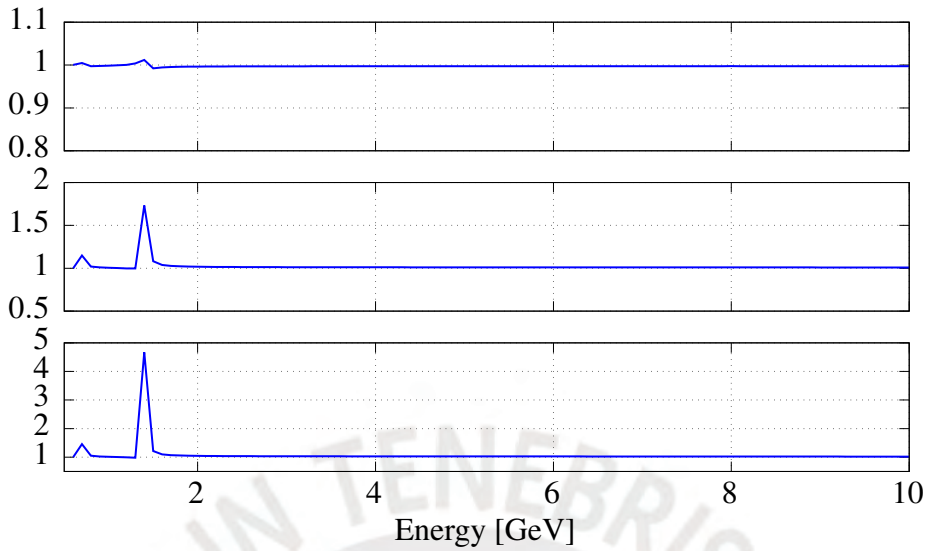

Figure 5.2: Probability ratios, $P_{Standard}/P_{NSI}$, for $\varepsilon_{\mu\tau}^{s/d} = 0.0018$ (top), $\varepsilon_{\mu e}^{s/d} = 0.0018$ (middle) and $\varepsilon_{\mu e}^{s/d} = 0.0046$ (bottom).

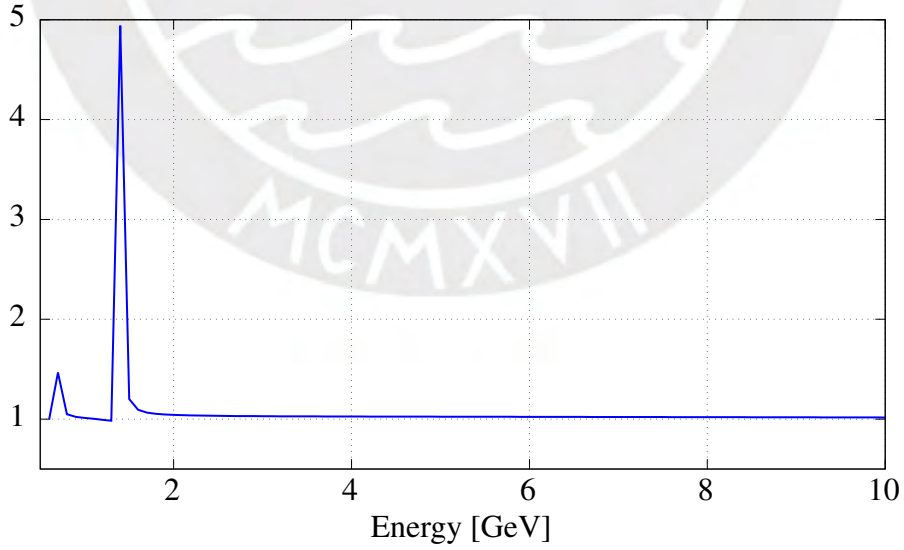

Figure 5.3: Probability ratio, $P_{Standard}/P_{NSI}$, for $\varepsilon_{\mu\tau}^{s/d} = 0.0018$ and $\varepsilon_{\mu e}^{s/d} = 0.0046$ combined.

With these values, the new (normalized) initial state ν_μ and final state ν_e were defined. We consider only vacuum oscillation and a 1300 km baseline. Figs. 5.2 and 5.3 show the appearance probability ratio, $P_{Standard}/P_{NSI}$, for different scenarios. First, we compare the effect of only one charged-current non-standard parameter: $\varepsilon^{s/d}_{\mu\tau} = 0.0018$, $\varepsilon^{s/d}_{\mu e} = 0.0018$ and $\varepsilon^{s/d}_{\mu e} = 0.0046$ in Fig. 5.2. The effect of the maximum value of both the parameters together ($\varepsilon^{s/d}_{\mu e} = 0.0046$ and $\varepsilon^{s/d}_{\mu\tau} = 0.0018$) in shown in Fig. 5.3.

Let us first comment on the impact of each of the parameters here considered. The top and middle plots in Fig. 5.2 include same magnitude NSI parameters, however the impact of the $\varepsilon_{\mu e}$ parameter has a clearly more relevant effect on the probability. The contribution of each parameter, when combined, then seem to add up.

Notice that for every scenario, the ratio stays close to 1 (it is actually $\pm 10^{-2}$ numerically) for most of the energy values, but for two very noticeable peaks. These appear at 0.7 and 1.4 GeV at ratios of 1.47 and 4.94 respectively. That is, the probability in the standard case is larger than the non-standard one. A couple of points can be made of this, using Eq. (4.17).

While there is an extra term adding to the probability that depends on the production/detection non-standard parameters, they also appear in the other terms. Particularly, they make the negative term more significant, as $\delta_{CP} = 0$ and our parameters are real. Furthermore, the energy values of the peaks approximately correspond to the lowest probability points for every case, exactly where the small valued terms in the equation play a more significant role. As also expected from the equation, the charged-current non-standard parameters do not

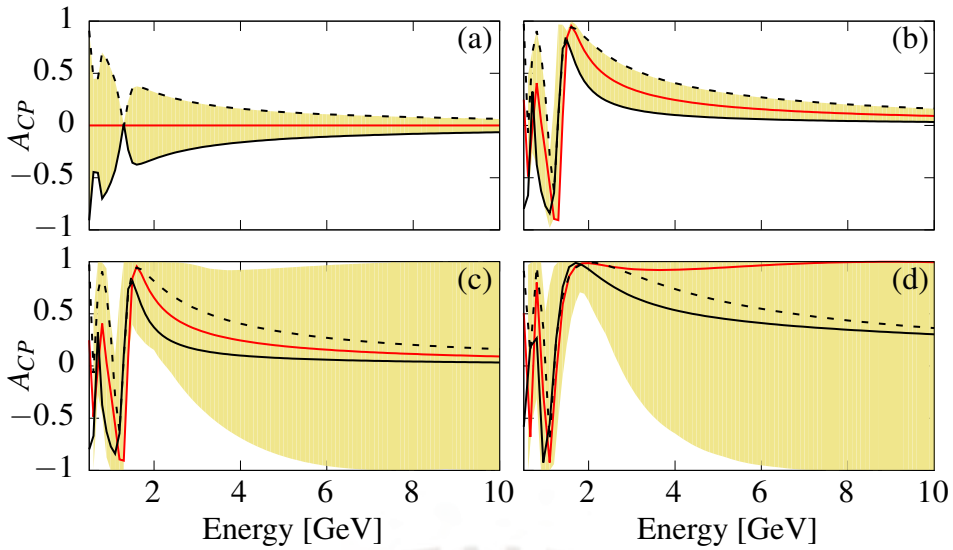

Figure 5.4: A_{CP} for a wide range of parameter values: a) Vacuum, varying δ_{CP}, b) standard interactions varying δ_{CP}, c) NSI varying with δ_{CP} and the moduli of ε_{ee}, $\varepsilon_{e\mu}$ and $\varepsilon_{e\tau}$, d) NSI with all moduli set to maximum, varying all phases.

change any phase in the oscillatory terms, only their amplitudes. So, the zero-distance effect would not necessarily lead to "enhanced" probabilities, these are just misleading.

5.4.2 Fake CP-violating signals

The definition of A_{CP} in Eq.(4.30) will now be used to show the possible effect on CP-violation observations of both standard and non-standard interactions in neutrino propagation through matter. The values were chosen arbitrarily and according to the constraints in section 5.4.2. Fig. 5.4 shows A_{CP} for the following cases:

(a) Vacuum oscillations considering $\delta_{CP} \in [0, 2\pi)$: The solid red line represents $\delta_{CP} = 0$, while the solid and dashed black lines represent $\delta_{CP} = \pi/2$ and $-\pi/2$ respectively.

(b) Oscillations in matter with standard oscillations: The lines correspond to the same values of δ_{CP}.

(c) Oscillations in matter adding Non-Standard Interactions, with $\varepsilon_{ee} \in [0, 1.5]$, $|\varepsilon_{e\mu}|$ and $|\varepsilon_{e\tau}|$ both in $[0, 0.15]$: The lines are the same as in the standard interaction case.

(d) Oscillations in matter with Non-Standard Interactions, with $\varepsilon_{ee} = 1.5$, $|\varepsilon_{e\mu}|, |\varepsilon_{e\tau}| = 0.15$, and all phases in $[0, 2\pi)$: The lines correspond to the same values of δ_{CP} as before, with present NSI parameters set to maximum.

As expected from Eq.(4.31), A_{CP} is zero when $\delta_{CP} = 0$ and it is maximized for $\delta_{CP} = \pi/2$ and $-\pi/2$ when there are no matter effects. However, the signal for all values of δ_{CP} drastically changes even with only standard interactions. Particularly, we are pointed towards a CP-violating signal even for $\delta_{CP} = 0$, and the parameters giving different maxima are not as clear as in the vacuum scenario. At the same time, the possible values of the asymmetry seem to be closer to a central value for all energies.

The effect of only the NSI moduli compared to the standard interaction case can be seen in plot c. Notice how the band is no longer constrained by curves corresponding to "maximum CP-violation". Instead, the asymmetry can take basically any (allowed) value for higher energies, unlike the vaccum case, where larger asymmetries are found for lower energies. From the curves in plot d, we can also see exactly how the NSI moduli affects specific signals: we no longer see the CP-conserving signal in-between $\delta_{CP} = \pi/2, -\pi/2$, but it becomes one

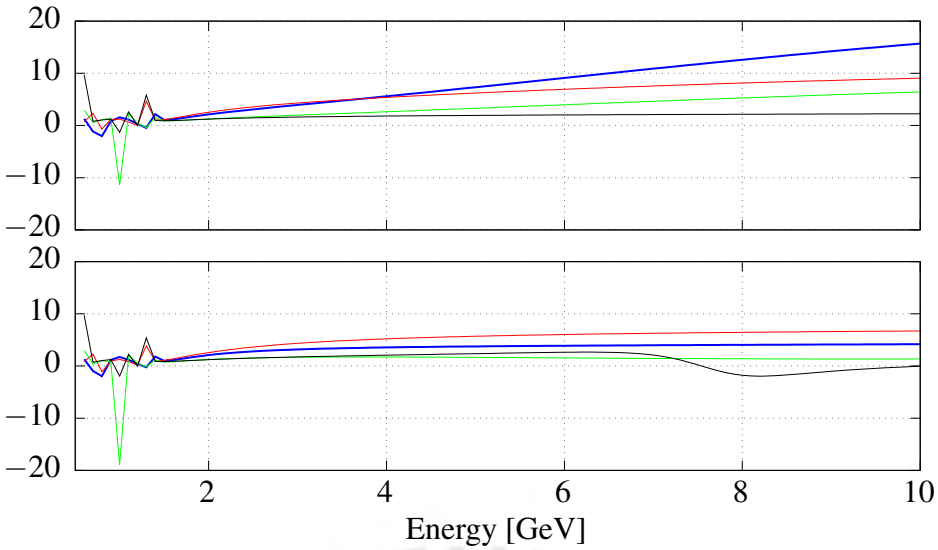

Figure 5.5: A_{CP} ratio for only NSI moduli (top), and NSI moduli and phases (bottom), for δ_{CP} values of $-\pi/2$ (black), $-\pi/4$ (green), $\pi/4$ (blue), and $\pi/2$ (red), compared to standard oscillations in matter.

of the cases for largest asymmetry. The effect of considering the NSI phases, finally, only make for an even wider band for all energies.

We now focus on CP-violating cases. Figs. 5.5 and 5.6 show the ratio of CP-asymmetry for fixed sets of parameters, where each plot includes curves for $\delta_{CP} = -\pi/2$ (black), $\delta_{CP} = -\pi/4$ (green), $\delta_{CP} = \pi/4$ (blue), and $\delta_{CP} = \pi/2$ (red). Apart from vacuum and standard oscillations in matter, we consider two cases of NSI with the moduli set to their respective maxima: one with no phases and another with NSI phases set to $\phi_{e\mu} = 1.5\pi$ and $\phi_{e\tau} = 1.6\pi$, as suggested in [45].

We first compare oscillations in matter, with the ratio $A_{CP,NSI}/A_{CP,standard}$ in Fig. 5.5. For NSI moduli (top) alone, the ratio is positive for most energy values in all cases, and can get up to about 16. On the other hand, CP-asymmetries seem to vary less when considering the NSI moduli and phases (bottom). However, the latter plot does include negative ratios for $\delta_{CP} = -\pi/2$ in the higher

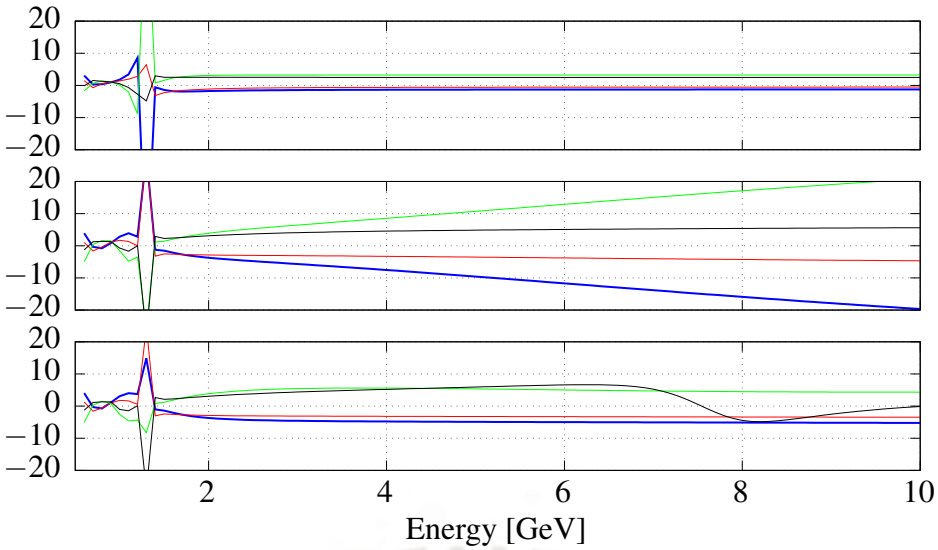

Figure 5.6: A_{CP} ratio for standard interactions (top), NSI moduli (middle) and NSI moduli and phases (bottom) compared to oscillations in vacuum.

energies, and it enhances the negative peak seen in the former. Thus, for these values of δ_{CP}, NSI moduli mostly contribute to CP-violation signals the same way standard oscillations do (A_{CP} for both standard and non-standard scenarios have the same sign), while NSI moduli and phases may contribute in the "opposite" way.

Fig. 5.6 shows A_{CP} for standard interactions (top), NSI moduli only (middle) and NSI moduli and phases (bottom), compared to oscillations in vacuum ($A_{CP,matter}/A_{CP,vacuum}$). It is more evident that matter effects play a large role when studying CP-violation signals, and even more so if Non-Standard Interactions are actually present. Very large peaks appear at about 1GeV, which suggests, for example, that maximizing A_{CP} by using low energies (see Eq.(4.31)) may only lead to a more misleading analysis of CP-violating parameters. Furthermore, while NSI parameters are added, the ratios follow more complicated patterns with δ_{CP}, rather than "signatures" for each case. Finally, the bottom

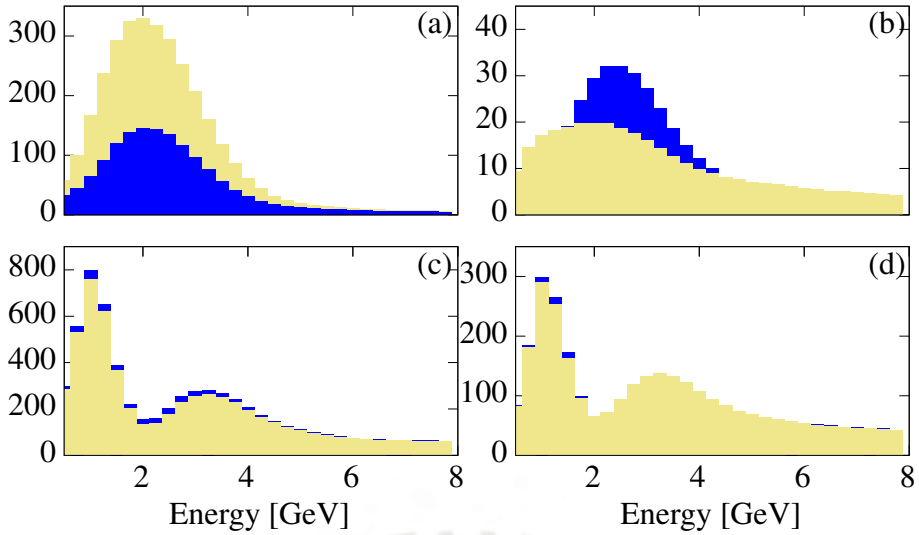

Figure 5.7: Event rates in bins of 0.25GeV for the channels: a) $\nu_\mu \to \nu_e$, b) $\bar{\nu_\mu} \to \bar{\nu_e}$, c) $\nu_\mu \to \nu_\mu$, d) $\bar{\nu_\mu} \to \bar{\nu_\mu}$ considering standard interactions (blue) and NSI (yellow).

plot basically represents ratios of possible signals in the experiments mentioned in section 5.5.3, and a discrepancy in their measurements may be more evident.

5.4.3 NSI at DUNE

We now turn to the effect of Non-Standard Interactions in event rates and following parameter fit in the context of DUNE. For the simulation, we consider 3.5 years in neutrino and antineutrino mode, fiducial detector mass of 40 kt and 1.07 MW beam power. All data was generated using normal mass hierarchy and no CP-violating phases (δ_{CP} and $\phi_{NSI} = 0$).

We show the event rates for Non-Standard Interactions, with $\varepsilon_{ee} = 1.5$, $\varepsilon_{e\mu}$ and $\varepsilon_{e\tau} = 0.15$ (yellow histogram), in contrast to the standard case (blue histogram) in Fig. 5.7. There is a very clear difference in event rates for more relevant energies (higher energies will have smaller flux either way) for both appearance channels (top histograms), and a shift of the peak specifically for antineutrino

appearance. On the other hand, disappearance channels (bottom histograms) show small differences that could very well be the result of statistical fluctuations. This is to be expected, as the choice of NSI parameters was driven by the leading order approximation of the appearance channels.

Channel	Standard	Only $\varepsilon_{e\mu} = 0.02$	Only $\varepsilon_{e\tau} = 0.02$
$\nu_\mu \to \nu_e$	1257 / 341	1335 / 340	1294 / 340
$\bar{\nu_\mu} \to \bar{\nu_e}$	277 / 199	266 / 199	276 / 199
$\nu_\mu \to \nu_\mu$	8263 / 106	8233 / 106	8253 / 106
$\bar{\nu_\mu} \to \bar{\nu_\mu}$	4140 / 60	4142 / 60	4140 / 60

Table 5.2: Signal/Background event rates for all scenarios considered in parameter fit.

To see the effect of NSI in parameter fit, we consider data generated with additional parameters, in two scenarios: one with only $\varepsilon_{e\mu} = 0.02$ and another with only $\varepsilon_{e\tau} = 0.02$. The binned event rates are not shown for these cases, as the differences with respect to the standard case are barely noticeable and only the $\bar{\nu_\mu} \to \bar{\nu_e}$ channel. The total event rates are shown in Table 5.2.

While our true data may include New Physics, the fit in every case is done considering only standard parameters and all of them are marginalized over to find the minimum χ^2. We also include Gaussian priors on $\sin^2\theta_{12}$, $\sin^2\theta_{13}$, $\sin^2\theta_{23}$ rather than those parameters themselves, and on both mass squared differences. To obtain the allowed regions, we consider:

$$\Delta\chi^2 = \chi^2 - \chi^2_{min} \tag{5.2}$$

where χ^2 is evaluated with all parameter set to their fit values, except for those

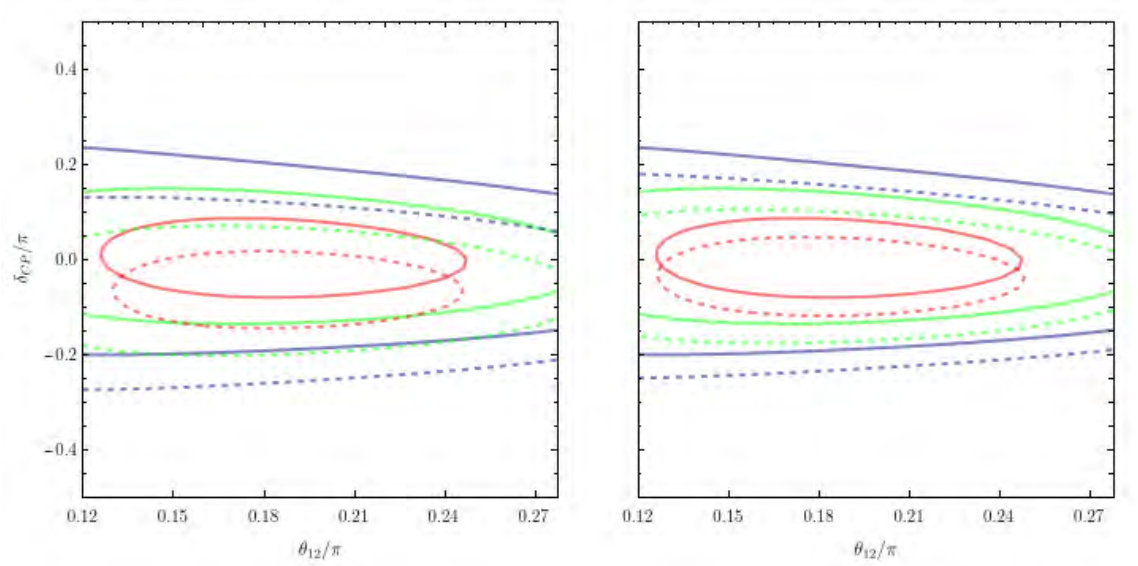

Figure 5.8: 1σ (red), 2σ (green) and 3σ (blue) allowed regions. Dashed lines correspond to true $\varepsilon_{e\mu} = 0.02$ on the left plot, and $\varepsilon_{e\tau} = 0.02$ on the right. Solid lines represent no true NSI parameter.

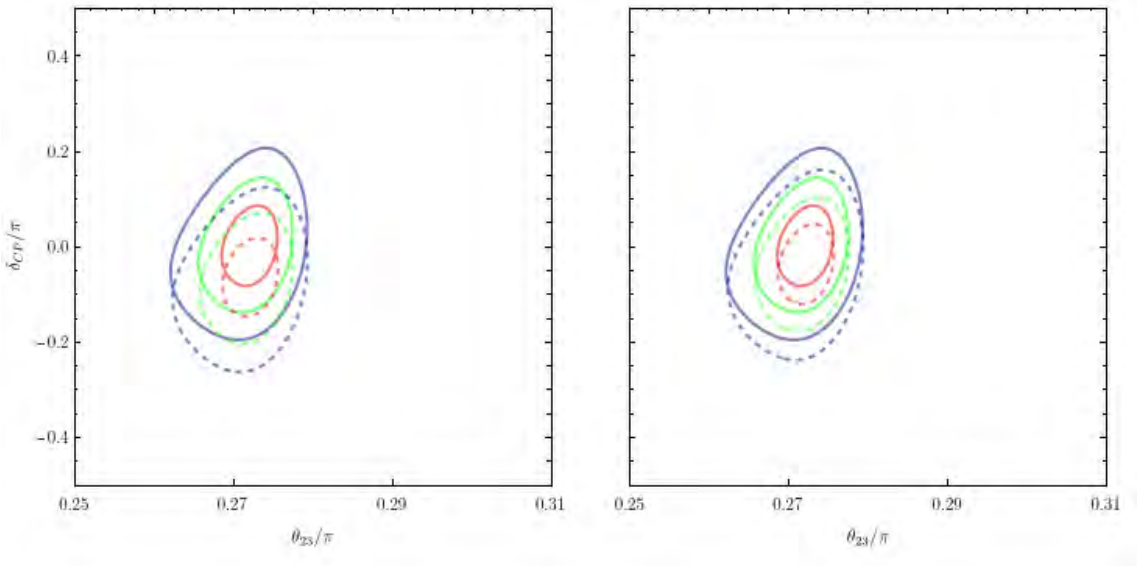

Figure 5.9: 1σ (red), 2σ (green) and 3σ (blue) allowed regions. Dashed lines correspond to true $\varepsilon_{e\mu} = 0.02$ on the left plot, and $\varepsilon_{e\tau} = 0.02$ on the right. Solid lines represent no true NSI parameter.

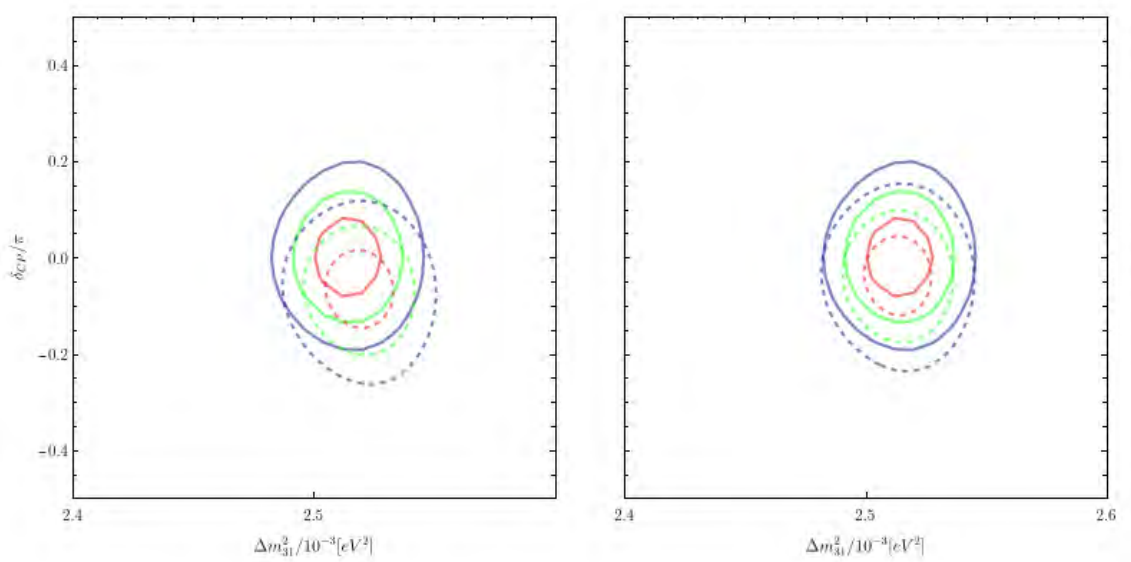

Figure 5.10: 1σ (red), 2σ (green) and 3σ (blue) allowed regions. Dashed lines correspond to true $\varepsilon_{e\mu} = 0.02$ on the left plot, and $\varepsilon_{e\tau} = 0.02$ on the right. Solid lines represent no true NSI parameter.

that appear on the respective plots (all parameters fixed), and we scan only over normal mass hierarchy.

Figs. 5.8, 5.9 and 5.10 show the allowed regions for a (seemingly) robust measured parameter, θ_{12}, and the parameters that allow degeneracies, θ_{23}, δ_{CP} and Δm^2_{31}. All regions agree on a clear shift towards lower values for δ_{CP}, even for these small values of NSI parameters that do not seem to have a large effect on event rates. The shift is of course more prominent when considering $\varepsilon_{e\mu}$, as $\varepsilon_{e\tau}$ would introduce some negative terms in the probability. Fit values of θ_{12} and θ_{23} are not affected by the introduction of NSI in Nature, although this is only when scanning normal hierarchy. On the other hand, the fit values of Δm^2_{31} do suffer a shift: smaller δ_{CP} and larger Δm^2_{31} are needed to balance the probability when considering the new interactions.

We finally obtain the sensitivity to CP-violation and mass hierarchy DUNE, with data generated as previously detailed. The sensitivity in each case is de-

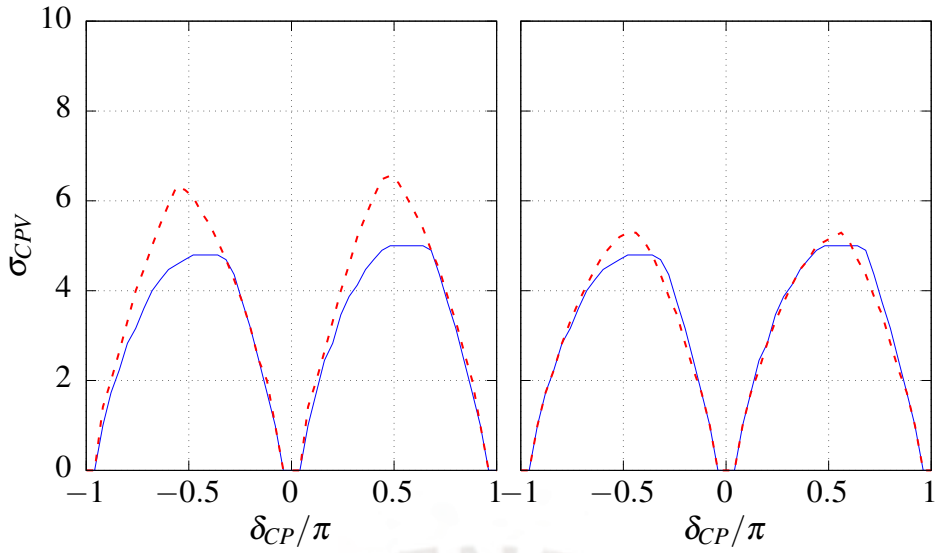

Figure 5.11: DUNE sensitivity to CP-violation when only standard (blue solid lines) and Non-Standard (red dashed lines) Interactions are present in Nature, for $\varepsilon_{e\mu} = 0.02$ (left) and $\varepsilon_{e\tau} = 0.02$ (right).

fined as [52]:

$$\begin{aligned}
\sigma_{CPV} &= \sqrt{\Delta\chi^2_{CPV}} \\
&= \sqrt{Min[\Delta\chi^2_{CP}(\delta^{test}_{CP} = 0), \Delta\chi^2_{CP}(\delta^{test}_{CP} = \pi)]}, \\
&\text{where} \quad \Delta\chi^2_{CP} = \chi^2_{\delta^{test}_{CP}} - \chi^2_{\delta^{true}_{CP}} \\
\sigma_{MH} &= \sqrt{\Delta\chi^2_{MH}} = \sqrt{\chi^2_{IH} - \chi^2_{NH}}
\end{aligned} \tag{5.3}$$

Figs. 5.11 and 5.12 show the sensitivity as functions of δ_{CP}, where the blue lines are those obtained with data generated with only standard parameters and the red lines correspond to $\varepsilon_{e\mu} = 0.02$ on the left and $\varepsilon_{e\tau} = 0.02$ on the right. It should be noted that, as mentioned in [57], there may be a decrease in sensitivity when adding more degrees of freedom (parameters to fit). However, our comparison only contemplates different sets of data rather than different fitted models. Thus, variations in σ_{CPV} or σ_{MH} should be attributed to the NSI parameters considered in every case.

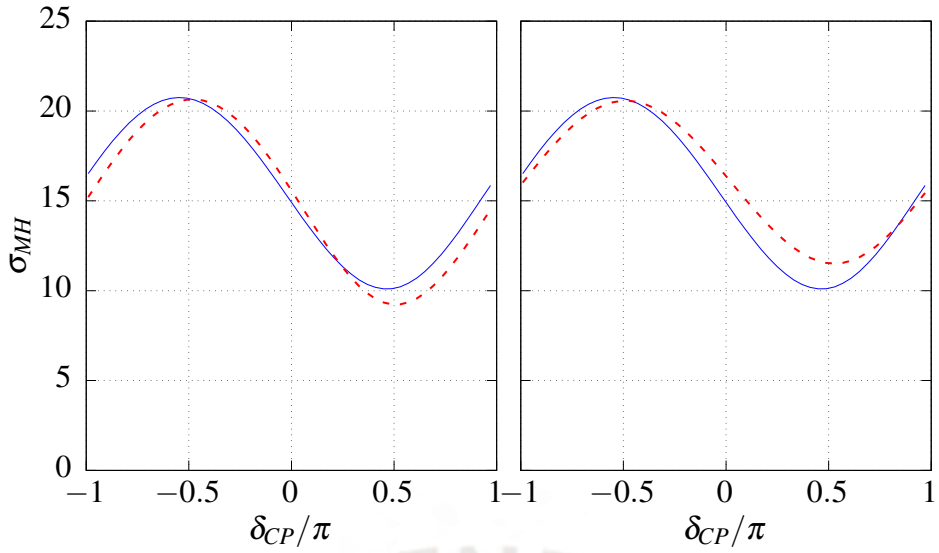

Figure 5.12: DUNE sensitivity to mass hierarchy when only standard (blue solid lines) and Non-Standard (red dashed lines) Interactions are present in Nature, for $\varepsilon_{e\mu} = 0.02$ (left) and $\varepsilon_{e\tau} = 0.02$ (right).

For the CP-violation sensitivity plot, we can only confirm the previous observations of A_{CP} in the presence of NSI. From Eq.(5.3), non-zero values of σ_{CP} imply that the data is in disagreement with a CP-conserving scenario and, while stronger non-standard parameters are added, the disagreement does become different from the standard case: the CP-asymmetry has changed. Furthermore, the disagreement becomes larger for most values of δ_{CP} and the effect is particularly relevant for maximum CP-violation.

Finally, the sensitivity to mass hierarchy hints at how certainly we could reject, in our case, the inverse hierarchy fit. The plots in Fig. 5.12 both show a slight shift in the values of δ_{CP}. The sensitivity remains at values close to the standard case, and may still allow the determinations of mass hierarchy. Notice, however, that the effect of each NSI parameters is not always to make σ_{MH} larger, and stronger parameters may lead to smaller significances than desired.

Chapter 6

Conclusions

Neutrino physics is currently a very active research field, which makes for interesting studies and an abundance of available information. In a context where increasingly complex models and hypotheses are being considered for describing neutrinos, some of their aspects may seem crystal clear. This could be the case for the widely accepted mass-induced neutrino oscillations and its quantum mechanics formulation. However, some details of it could lead to inconsistencies, and have been discussed in this work in order to settle the robustness of the formalism. Furthermore, while neutrino mass itself is proof of Physics Beyond the Standard Model, we inquire about one possible consequence of it: Non-Standard Neutrino Interactions with matter (NSI). We have reviewed the introduction of NSI in the established formalism and its impact on neutrino propagation, in an attempt to create a formidable starting point for further research.

Neutrino oscillations are the periodic change in flavor as the result of quantum interference between neutrino mass states and it is logical to express flavor states as superpositions of the latter. The (evolving) mass states must be

represented by wave packets, so they can in fact account for both the localization of the particle and its corresponding quantum uncertainties. The approach also clarifies the conditions for observing the oscillations in experiments and leads to the coherence conditions. However, the plane wave approach, which is commonly used and is found to include some inconsistencies, also seems to give correct results. This can be explained by the fact that the approximations used here correspond to the coherence conditions. As oscillation probabilities are found to be Lorentz-invariant, the description of neutrino oscillations then seems to be consistent.

Interactions of neutrinos with matter were then considered and the differential equation to be solved was found, all following Standard Model processes. We have then focused on the possibility that Non-Standard Interactions may as well be present in Nature and how it is usually included in the equations. It is noted that NSI may be neutral or charged-current processes. They affect not only propagation, but also neutrino production and detection, although with different strengths according to theoretical and experimental constraints.

Some relevant effects of Non-Standard Interactions were presented. For charged-current NSI, the most notable effect is neutrino production (or detection for that matter) of unexpected flavors. This could wrongfully contribute to oscillation observations, although not necessarily enhance flavor conversion. For neutrino propagation, the effects become more complex.

We have evaluated Non-Standard Interactions in the Deep Underground Neutrino Experiment (DUNE), as its 1300 km baseline allows matter effects that make for large CP-asymmetry. It is expected to not only measure δ_{CP} pre-

cisely, but also determine the mass hierarchy. When including NSI in Nature, parameter fit is shown to be affected, particularly for the CP-violating phase, and experiment sensitivities change.

Finally, we would like to mention that, while matter effects in general lead to fake CP-violating signals, DUNE does not aim to determine δ_{CP} from the CP-asymmetry. It aims to observe the agreement between the measured phase and A_{CP}, which will allow potential for the study of Physics Beyond the Standard Model. However, NSI are not the only possible phenomenon, and evaluating them in the context of one experiment will not suffice. As noted in [58], testing frameworks call for an agreement and consistency in the results of different experiments, model-independent parametrization of the phenomena, and subsequently considering specific models to identify new signatures. Ultimately, achieving precision in the measurement of parameters in all experiments and the collaboration between them is of utmost importance.

Bibliography

[1] A. PÉREZ GARCÍA, 2020. "Revisión teórica de oscilaciones de neutrinos". Tesis de grado - PUCP.

[2] C. GIUNTI, W. CHUNG, 2007. "Fundamentals of neutrino physics and astrophysics". *Fundamentals of Neutrino Physics and Astrophysics, by Carlo Giunti and W. Kim Chung. ISBN 978-0-19-850871-7 (HB). Published by Oxford University Press, Oxford, Great Britain, 2007.* .

[3] V. NESVIZHEVSKY, J. VILLAIN, 2017. "The discovery of the neutron and its consequences (19301940)". *Comptes Rendus Physique 18*(9):592 . ISSN 1631-0705. URL `http://www.sciencedirect.com/science/article/pii/S1631070517300993`.

[4] H.-K. QUANG, X.-Y. PHAM, 1998. Elementary particles and their interactions: concepts and phenomena. ISBN 9783642083495.

[5] M. ALTMANN, ET AL., 2001. "Solar neutrinos". *Rep. Prog. Phys 64*:97.

[6] A. DAR, G. SHAVIV, 1999. "The Solar neutrino problem: An Update". *Phys. Rept. 311*:115. `astro-ph/9808098`.

[7] C. GRUPEN, 2005. Astroparticle Physics. Springer. URL `https://www.xarg.org/ref/a/B001089JM6/`.

[8] Y. FUKUDA, ET AL. (Super-Kamiokande), 1998. "Evidence for oscillation of atmospheric neutrinos". *Phys. Rev. Lett. 81*:1562. `hep-ex/9807003`.

[9] D. KRUPPKE, 2007. On Theories of Neutrino Oscillations: A Summary and Characterisation of the Problematic Aspects. Proyecto Fin de Carrera, Bielefeld U.

[10] C. GIUNTI, C. W. KIM, 2001. "Quantum mechanics of neutrino oscillations". *Found. Phys. Lett. 14*(3):213. `hep-ph/0011074`.

[11] E. AKHMEDOV, 2019. "Quantum mechanics aspects and subtleties of neutrino oscillations". En "International Conference on History of the Neutrino: 1930-2018 Paris, France, September 5-7, 2018", `1901.05232`.

[12] Y. GROSSMAN, H. J. LIPKIN, 1997. "Flavor oscillations from a spatially localized source: A Simple general treatment". *Phys. Rev. D55*:2760. `hep-ph/9607201`.

[13] C. GIUNTI, 2001. "Energy and momentum of oscillating neutrinos". *Mod. Phys. Lett. A16*:2363. `hep-ph/0104148`.

[14] B. KAYSER, 1981. "On the Quantum Mechanics of Neutrino Oscillation". *Phys. Rev. D24*:110.

[15] K. KIERS, N. WEISS, 1998. "Neutrino oscillations in a model with a source and detector". *Phys. Rev. D57*:3091. hep-ph/9710289.

[16] C. GIUNTI, 2004. "Lorentz invariance of neutrino oscillations". *American Journal of Physics 72*(5):699. https://doi.org/10.1119/1.1643372, URL https://doi.org/10.1119/1.1643372.

[17] V. A. BEDNYAKOV, D. V. NAUMOV, 2019. "On coherent neutrino and antineutrino scattering off nuclei". 1904.03119.

[18] J. LINDER, 2005. "Derivation of neutrino matter potentials induced by earth" hep-ph/0504264.

[19] M. TANABASHI, ET AL. (Particle Data Group), 2018. "Review of particle physics". *Phys. Rev. D 98*:030001. URL https://link.aps.org/doi/10.1103/PhysRevD.98.030001.

[20] A. YU. SMIRNOV, 2003. "The MSW effect and solar neutrinos". En "Neutrino telescopes. Proceedings, 10th International Workshop, Venice, Italy, March 11-14, 2003. Vol. 1+2", págs. 23–43. hep-ph/0305106.

[21] L. WOLFENSTEIN, 1978. "Neutrino oscillations in matter". *Phys. Rev. D 17*:2369. URL https://link.aps.org/doi/10.1103/PhysRevD.17.2369.

[22] A. GAGO, ET AL., 2001. "Probing flavor changing neutrino interactions using neutrino beams from a muon storage ring". *Phys. Rev. D 64*:073003. hep-ph/0105196.

[23] A. GAGO, ET AL., 2010. "Resolving CP Violation by Standard and Nonstandard Interactions and Parameter Degeneracy in Neutrino Oscillations". *JHEP 01*:049. 0904.3360.

[24] S. BERGMANN, A. KAGAN, 1999. "Z - induced FCNCs and their effects on neutrino oscillations". *Nucl. Phys. B 538*:368. hep-ph/9803305.

[25] J. SCHECHTER, J. W. F. VALLE, 1980. "Neutrino masses in su(2) $\otimes$ u(1) theories". *Phys. Rev. D 22*:2227. URL https://link.aps.org/doi/10.1103/PhysRevD.22.2227.

[26] B. DEV, ET AL., 2019. "Neutrino non-standard interactions: A status report". *SciPost Physics Proceedings* (2). ISSN 2666-4003. URL http://dx.doi.org/10.21468/SciPostPhysProc.2.001.

[27] J. LIAO, ET AL., 2016. "Degeneracies in long-baseline neutrino experiments from nonstandard interactions". *Phys. Rev. D 93*:093016. URL https://link.aps.org/doi/10.1103/PhysRevD.93.093016.

[28] C. BIGGIO, ET AL., 2009. "General bounds on non-standard neutrino interactions". *JHEP 08*:090. 0907.0097.

[29] Y. GROSSMAN, 1995. "Nonstandard neutrino interactions and neutrino oscillation experiments". *Phys. Lett. B 359*:141. hep-ph/9507344.

[30] D. MELONI, ET AL., 2010. "Non-standard interactions versus non-unitary lepton flavor mixing at a neutrino factory". *JHEP 04*:041. 0912.2735.

[31] T. OHLSSON, H. ZHANG, 2009. "Non-Standard Interaction Effects at Reactor Neutrino Experiments". *Phys. Lett. B 671*:99. 0809.4835.

[32] S. K. AGARWALLA, ET AL., 2015. "Probing Non-Standard Interactions at Daya Bay". *JHEP 07*:060. 1412.1064.

[33] T. OHLSSON, 2013. "Status of non-standard neutrino interactions". *Rept. Prog. Phys. 76*:044201. 1209.2710.

[34] E. FERNANDEZ-MARTINEZ, 2011. "Non-standard neutrino interactions". *PoS HQL2010*:056.

[35] Y. FARZAN, M. TORTOLA, 2018. "Neutrino oscillations and Non-Standard Interactions". *Front. in Phys. 6*:10. 1710.09360.

[36] I. ESTEBAN, ET AL., 2018. "Updated Constraints on Non-Standard Interactions from Global Analysis of Oscillation Data". *JHEP 08*:180. 1805.04530.

[37] G. BARENBOIM, ET AL., 2019. "New physics vs new paradigms: distinguishing CPT violation from NSI". *Eur. Phys. J. C 79*(5):390. 1804.05842.

[38] M. GHOSH, ET AL., 2016. "New look at the degeneracies in the neutrino oscillation parameters, and their resolution by T2K, NOνA and ICAL". *Phys. Rev. D 93*(1):013013. 1504.06283.

[39] H. MINAKATA, H. NUNOKAWA, 1997. "How to measure CP violation in neutrino oscillation experiments?" *Phys. Lett. B 413*:369. hep-ph/9706281.

[40] T. KIKUCHI, ET AL., 2009. "Perturbation theory of neutrino oscillation with nonstandard neutrino interactions". *Journal of High Energy Physics 2009*(03):114114. ISSN 1029-8479. URL http://dx.doi.org/10.1088/1126-6708/2009/03/114.

[41] B. AHARMIM, ET AL., 2005. "Electron energy spectra, fluxes, and day-night asymmetries of8b solar neutrinos from measurements with nacl dissolved in the heavy-water detector at the sudbury neutrino observatory". *Physical Review C 72*(5). ISSN 1089-490X. URL http://dx.doi.org/10.1103/PhysRevC.72.055502.

[42] O. MIRANDA, ET AL., 2006. "Are solar neutrino oscillations robust?" *JHEP 10*:008. hep-ph/0406280.

[43] P. COLOMA, 2016. "Non-Standard Interactions in propagation at the Deep Underground Neutrino Experiment". *JHEP 03*:016. 1511.06357.

[44] M. BASS, ET AL., 2015. "Baseline Optimization for the Measurement of CP Violation, Mass Hierarchy, and θ_{23} Octant in a Long-Baseline Neutrino Oscillation Experiment". *Phys. Rev. D 91*(5):052015. 1311.0212.

[45] P. B. DENTON, ET AL., 2020. "CP-Violating Neutrino Non-Standard Interactions in Long-Baseline-Accelerator Data" 2008.01110.

[46] S. S. CHATTERJEE, A. PALAZZO, 2020. "Non-standard neutrino interactions as a solution to the NOνA and T2K discrepancy" 2008.04161.

[47] M. MASUD, ET AL., 2016. "Probing CP violation signal at DUNE in presence of non-standard neutrino interactions". *J. Phys. G 43*(9):095005. 1510.08261.

[48] E. JONES, ET AL., 2001–. "SciPy: Open source scientific tools for Python". [Online; accessed], URL http://www.scipy.org/.

[49] I. ESTEBAN, ET AL., 2020. "The fate of hints: updated global analysis of three-flavor neutrino oscillations". *JHEP 09*:178. 2007.14792.

[50] P. HUBER, ET AL., 2007. "New features in the simulation of neutrino oscillation experiments with GLoBES 3.0: General Long Baseline Experiment Simulator". *Comput. Phys. Commun. 177*:432. hep-ph/0701187.

[51] P. HUBER, ET AL., 2005. "Simulation of long-baseline neutrino oscillation experiments with GLoBES (General Long Baseline Experiment Simulator)". *Comput. Phys. Commun. 167*:195. hep-ph/0407333.

[52] R. ACCIARRI, ET AL. (DUNE), 2015. "Long-Baseline Neutrino Facility (LBNF) and Deep Underground Neutrino Experiment (DUNE): Conceptual Design Report, Volume 2: The Physics Program for DUNE at LBNF" 1512.06148.

[53] K. HUITU, ET AL., 2016. "Constraining the nonstandard interaction parameters in long baseline neutrino experiments". *Phys. Rev. D 93*(5):053016. 1601.07730.

[54] T. ALION, ET AL. (DUNE), 2016. "Experiment Simulation Configurations Used in DUNE CDR" 1606.09550.

[55] A. M. DZIEWONSKI, D. L. ANDERSON, 1981. "Preliminary reference earth model". *Physics of the Earth and Planetary Interiors 25*(4):297 . ISSN 0031-9201.

[56] A. GIARNETTI, D. MELONI, 2020. "Probing Source and Detector NSI parameters at the DUNE Near Detector" 2005.10272.

[57] M. MASUD, P. MEHTA, 2016. "Nonstandard interactions spoiling the *cp* violation sensitivity at dune and other long baseline experiments". *Phys. Rev. D 94*:013014. URL https://link.aps.org/doi/10.1103/PhysRevD.94.013014.

[58] I. MOCIOIU, 2020. "Long baseline neutrino oscillation phenomenology". Talk given at the XXIX International Conference on Neutrino Physics and Astrophysics, URL https://conferences.fnal.gov/nu2020/.